Hydrologic Scales, Cloud Variability, Remote Sensing, and Models: Implications for Forecasting Snowmelt and Streamflow

JAMES J. SIMPSON

Digital Image Analysis Laboratory, Scripps Institution of Oceanography, University of California, San Diego, La Jolla, California

MICHAEL D. DETTINGER

U.S. Geological Survey and Scripps Institution of Oceanography, University of California, San Diego, La Jolla, California

FRANK GEHRKE

Department of Water Resources, State of California, Sacramento, California

TIMOTHY J. MCINTIRE

Digital Image Analysis Laboratory, Scripps Institution of Oceanography, University of California, San Diego, La Jolla, California

GARY L. HUFFORD

National Weather Service, Anchorage, Alaska

ABSTRACT

Accurate prediction of available water supply from snowmelt is needed if the myriad of human, environmental, agricultural, and industrial demands for water are to be satisfied, especially given legislatively imposed conditions on its allocation. Robust retrievals of hydrologic basin model variables (e.g., insolation or areal extent of snow cover) provide several advantages over the current operational use of either point measurements or parameterizations to help to meet this requirement. Insolation can be provided at hourly time scales (or better if needed during rapid melt events associated with flooding) and at 1-km spatial resolution. These satellite-based retrievals incorporate the effects of highly variable (both in space and time) and unpredictable cloud cover on estimates of insolation. The insolation estimates are further adjusted for the effects of basin topography using a high-resolution digital elevation model prior to model input. Simulations of two Sierra Nevada rivers in the snowmelt seasons of 1998 and 1999 indicate that even the simplest improvements in modeled insolation can improve snowmelt simulations, with 10%–20% reductions in root-mean-square errors. Direct retrieval of the areal extent of snow cover may mitigate the need to rely entirely on internal calculations of this variable, a reliance that can yield large errors that are difficult to correct until long after the season is complete and that often leads to persistent underestimates or overestimates of the volumes of the water to operational reservoirs. Agencies responsible for accurately predicting available water resources from the melt of snowpack [e.g., both federal (the National Weather Service River Forecast Centers) and state (the California Department of Water Resources)] can benefit by incorporating concepts developed herein into their operational forecasting procedures.

1. Introduction

a. Importance of snowpack/snowmelt

More than one-half of the world's human population relies on freshwater runoff from mountains (Liniger et al. 1998), making variations and trends in the outflow from mountainous regions a primary social concern. In many regions, this outflow is dominated, at least part of each year, by highly variable melting snow. In the western United States, for example, mountain-basin peak snow accumulation exhibits significant variability, from ~20% to >200%, expressed as a percent of the average peak snow accumulation. Thus, there is a need to forecast accurately the available water supply from highly variable snowmelt if the myriad needs (human, environmental, agricultural, industrial) are to be satisfied, especially given legislatively imposed conditions

Corresponding author address: Dr. James J. Simpson, Digital Image Analysis Laboratory, Scripps Institution of Oceanography, University of California, San Diego, La Jolla, CA 92093.
E-mail: jsimpson@ucsd.edu

on water resource allocation. In some cases, this need implies near-real-time prediction requirements (e.g., floods).

Water supply forecasts are used in general terms for three broad areas of water management: hydroelectric power generation, storage and flood control reservoir operations, and environmental management (Table 1). Decisions made both in hydroelectric power and reservoir operation consider a range of forecast possibilities and different sensitivities to forecast inaccuracy. The effect of forecast uncertainty may be masked by other factors, and operations can be modified as this uncertainty manifests itself during the season.

The Sacramento–San Joaquin delta, for example, is an environmentally sensitive area that also serves as part of the conveyance for much of the water distributed by both the California Department of Water Resources State Water Project and the U.S. Bureau of Reclamation Central Valley project. Average water-year outflow for the system is 22.40×10^9 m³ [18.15 million acre feet (MAF)] for the four northern drainages and 7.33×10^9 m³ (5.94 MAF) for the four southern drainages. This flow amount is approximately one-third of the estimated total statewide surface runoff.

In an attempt to protect water quality and quantity in the delta, the State Water Resources Control Board has adopted an evolving set of managerial strategies. An important facet to these strategies has been the development of various year types relating to forecast water-year flows. The water-year type for determination of environmental standards is set for the months of February–April based on the forecast for conditions as of the first of the month. The forecast for conditions as of 1 May determines the water-year type for May through the following January.

Of the year types (critical, dry, below normal, above normal, and wet), the critical and dry years have sensitive outflow requirements. The dilemma for forecasting is that this type of change is based on a threshold value. A forecast of 6.72×10^9 m³ (5.45 MAF) for the Sacramento Valley water-year-type index would put the year into the dry category, and a value of 6.66×10^9 m³ (5.4 MAF) would result in assignment to the critical category. If the forecast inaccuracy were to result in a year-type determination of dry when in fact the year was critical, then the value of the additional 344×10^6 m³ (0.279 MAF) that erroneously would have to be released to meet regulatory requirements would be close to $150 million. Other changes in environmental requirements triggered by the water-year type can exacerbate the economic impact.

Numerous similar situations exist in upstream watersheds. Watersheds, for example, that have environmental issues (e.g., fisheries, forestry) can be affected by similar thresholds. If water is diverted, released, or stored unnecessarily (e.g., because of forecast error), then the downstream needs might not be met (no replacement water is available) or the replacement water

may be costly. Over 60 regulations and projects are directly affected by California Department of Water Resources streamflow forecasts each spring, with concerns ranging from floods and safety, environmental management, economic impacts and losses, to hydropower generation (Table 1). The same forecasts are the basis for an increasing number of less direct or regulatory uses. Moreover, a growing number of other agencies are making their own forecasts for internal use.

Improved inputs to hydrologic basin models, coupled with a new generation of high-spatial-resolution models, should provide a basis for significantly reducing the error between observed and model streamflow. Improved water supply forecasts will alleviate some of the uncertainty (and related environmental and economic harm) discussed above.

b. Scale issues in snowpack/snowmelt hydrology

Understanding of variations of mountain snowpacks, and of the timing and amounts of snowmelt that feeds mountain rivers, has grown in recent decades but still is impeded by difficult issues of scale. There are mismatches between the temporal and spatial scales of observation and the scales over which snowpacks and runoff vary, as well as mismatches between the scales at which we can describe climatic influences on snowpack formation and decline and the scales over which snowmelt contributions accumulate to form the overall discharge from river basins.

The physical processes that determine the timing and volumes of snowpack accumulation and ablation, including snowmelt, vary on a wide range of spatial and temporal scales (see Fig. 1 in Walker et al. 2001). The precipitation fields that deposit snow are essentially fractal in their distributions, varying at all spatial scales from 10s and 100s of kilometers to meters and less. The land surfaces that accumulate the snowpacks likewise vary at spatial scales from millimeters to 100s of kilometers. The metamorphosis of the snowpacks, from pure snow into mostly ice, and then eventually into liquid snowmelt, is forced by temperature, solar radiation, winds, and humidities. These climatic conditions also fluctuate on a wide range of spatial and temporal scales. Thus, the streamflow generated by snowmelt is the product of physical (and biological) processes that work over a broad range of spatial and temporal scales.

Winter precipitation varies in space because of differing orographic and dynamical uplifts as storms cross the mountains of the West (Alpert 1986; Hay and McCabe 1998; Pandey et al. 2000), from the scales of mountain ranges to less than a kilometer (e.g., Daly et al. 1994; Colle and Mass 1996). The spatial distribution of precipitation varies from storm to storm, as well as during storms, depending on the history, wind (propagation speeds and directions), and atmospheric (moist thermodynamic) conditions within the storms (Pandey et al. 1999). On longer time scales, the "typical" storm

histories, directions, and conditions also vary with the states of the regional and global climate systems [e.g., from El Niños to La Niñas and on the longer interdecadal scales of the North Pacific climate system (Cayan and Webb 1992; Mantua et al. 1997)]. Winds, temperatures, and other climatic conditions, during and between storms, also vary erratically in high-mountain environments (Greenland and Losleben 2001).

Spatial accumulations of snow depend on the original precipitation distribution and on the distributions of shelter from winds and thermal conditions across the landscape. As a result, snow cover and thickness vary from windswept clearings (fell fields) to snow beds of considerable depth over distances ranging from meters to kilometers (Betterton 2001; Walker et al. 2001). Avalanches, both large and small, modify the spatial distributions of snow quickly (Mock and Birkeland 2000), and variations in the densities and kinds of vegetation can interact with the snowpack persistently to modify or to determine where snow accumulates (e.g., Armstrong 1988; Nakai et al. 1999). Upon accumulation, snowpack heat and moisture balances and, eventually, snowmelt vary widely from place to place and (of course) from range to range (e.g., Kattelman and Elder 1993; Tarboton et al. 1995), in response to permanent and transient climatic (and microclimatic) differences, often associated with complex terrain, shading by terrain and vegetation, and other local factors. In addition to these ''fixed'' conditions, each day (and season) brings variations in temperature, cloud cover, and wind that influence (from above) both the location and the evolution of the snowpack and snowmelt on mountainous terrains. Thus, the distributions of snowpack and snow cover are highly variable over an enormous range of time and space scales (e.g., Robinson and Dewey 1990; Hardy et al. 1998; Elder et al. 1998; Betterton 2001).

The hydrologic results of these spatially and temporally varying land surface and climate conditions are complex differences and changes in snowmelt, soil moisture, and streamflow across the snow-covered mountain watersheds of the West (Elder et al. 1998; Harrington and Bales 1998; Peterson et al. 2000; Lundquist and Cayan 2002). As a consequence, understanding, observing, and predicting such variations are central goals for hydrologists and resource managers alike in snow-dominated and snowfed regions of the world (e.g., Bales and Harrington 1995; Hardy et al. 1998).

The subsets of scales represented by observations and models are, each, inevitably small parts of the full range of variations. Thus, the most pressing need is to devise strategies for making measurements and simulations that represent the real-world results of snowpack variations at practical scales. Blöschl (1999, p. 2150) argued that the primary problem associated with scale in snowpack hydrology (indeed, the overarching problem in snow hydrology) is that ''the scale at which data are collected is different from the scale at which predictions are needed.''

c. Models of snowpack/snowmelt hydrological behavior

In the past, simulations and predictions of snowpacks and snowmelt runoff have confronted the issue of scale in snow hydrology with differing strategies. In broad terms, many models have resorted to coarse spatial lumping of processes and observations, others have treated snow variations as stochastic processes, and still others have simulated variations at or below the smallest scales of observation. In most cases, elevation is the primary basin characteristic accommodated by the models because of the strong control that it exerts on temperatures and, often, winter precipitation. In 1986, for example, an international survey of 11 snowmelt-runoff models (World Meteorological Organization 1986) showed that 9 of the 11 models subdivided basins into broad elevation zones. Of note, most of the models compared at that time still are in wide use in both operational and research settings. Only two models [Precipitation-Runoff Modeling System (PRMS) and Institute of Hydrology Distributed Model; see Leavesley et al. (1983) and Beven et al. (1987), respectively] allowed other details of the topography, soils, and land surfaces to determine snowpack/snowmelt characteristics and processes. Several of the elevationally lumped models represented large river basins by only two zones: a high-elevation snowpack-dominated zone and a low-elevation rainfall-dominated zone (e.g., the National Weather Service Sacramento River Modeling System). Even in the fully distributed models, the spatial distribution of meteorological conditions within the model is often specified in terms of elevational differences (e.g., Leavesley et al. 1983).

The meteorological inputs that the models are designed to accept are primarily those that have historically been available in practice for high-mountain watersheds: most common, temperature and precipitation. Thus, in the 1986 survey, the meteorological inputs for the models include temperature and precipitation in all cases and then, less common, evaporation potential (in four models), snowpack water content (in two models), and snow cover (in one model). Because insolation observations are not common within mountain basins, except in a relatively few research parks, the models have not usually required, or accepted, them as input. Among the models surveyed in 1986, only the PRMS (Leavesley et al. 1983) was designed to allow incorporation of observed or estimated insolation rates, even though snowmelt is largely fueled by insolation (Aguado 1985). In a similar way, in response to the historical lack of data from within most modeled basins, the models typically simulated (and were calibrated in terms of) streamflow at the outlet of a river basin, with no clear avenues for incorporating observations of snow or hydrologic variations elsewhere within the basins.

Recent models (e.g., Kirnbauer et al. 1994; Tarboton et al. 1995; Lohmann et al. 1998; Marks et al. 1999)

TABLE 1. Regulation or project affected by the State of California Department of Water Resources (DWR) forecast showing the agencies affected and the major concern [i.e., safety, environmental (envir.), or economic (econ.)]. Here WQ = water quality, ROD = record of decision, SF = South Fork, MF = Middle Fork, NF = North Fork, BLM = Bureau of Land Management, WY = water year, WA = water agency(-ies), AJ = Apr–Jul, WSD = watershed district, and Sac. = Sacramento. Other terms are defined in the table.

Regulation/project	DWR forecast	Agencies affected	Major concern (Safety/envir./econ.)
U.S. Army Corps of Engineers (USACE) flood control requirements (flood control diagram snowmelt parameter)			Also hydropower
Camanche storage	Mokelumne AJ forecast	USACE, East Bay Municipal Utility District (MUD)	Safety, econ.
New Melones storage	Stanislaus AJ forecast	USACE, Central Valley Project (CVP)	Safety, econ.
New Don Pedro storage	Tuolumne AJ forecast	USACE, Modesto Irrigation District (ID), Turlock ID	Safety, econ.
Exchequer storage	Merced AJ forecast	USACE, Merced ID	Safety, econ.
Millerton storage	San Joaquin (SJ) AJ forecast	USACE, CVP	Safety, econ.
Pine Flat storage	Kings AJ forecast	USACE, Kings River Conservation District (CD) and WA	Safety, econ.
Terminus storage	Kaweah AJ forecast	USACE, Kaweah Delta Water Conservation District (WCD)	Safety, econ.
Success storage	Tule AJ forecast	USACE, Tule River Association	Safety, econ.
Isabella storage	Kern AJ forecast	USACE, Kern agencies	Safety, econ.
Environmental Regulations			
State Water Resources Control Board (SWRCB), decision No.			
Sac.–SJ delta flow and WQ (D-1641)	Sac. valley index	SWRCB, State Water Project (SWP), CVP	Envir., econ.
Sac.–SJ delta flow and WQ (D-1641 & 1485)	Sac. river index	SWRCB, SWP, CVP	Envir., econ.
Sac.–SJ delta flow and WQ (D-1641)	8 river index	SWRCB, SWP, CVP	Envir., econ.
SJ river flow and WQ (D-1641)	SJ index	SWRCB, SWP, CVP	Envir., econ.
SJ river flow (D-1641)	SJ index	SWRCB, Merced ID, Turlock ID, Modesto ID, Oakdale ID	Envir., econ.
Mokelumne releases (D-1641)	Mokelumne WY forecast	SWRCB, East Bay MUD	Envir., econ.
Mokelumne releases (D-1641)	Mokelumne WY forecast	SWRCB, Woodbridge ID	Envir., econ.
Yuba releases (D-1644)	Yuba river index	SWRCB, Yuba Country WA	Envir., econ.
Environmental decisions (1993 winter-run biological opinion, 2000 Trinity River mainstem fishery ROD, 1983 CDFG agreement):			
Trinity releases	Trinity WY forecast	CVP	Envir., econ.
Sacramento river temperatures	Sac. river index	CVP, U.S. Fish and Wildlife Service (USFWS)	Envir., econ.
Wilkins "navigation" flow	Shasta WY forecast	CVP	Envir., econ.
Feather river flow	Feather AJ obs and forecast	SWP, CA Dept. of Fish and Game (CDFG)	Envir., econ.
CVP Improvement Act			
Vernalis adaptive management	Stanislaus—SJ monthly forecasts	CVP, Modesto ID, Turlock ID, Merced ID	Envir., econ.
Environmental water account	SWP allocation (indirect)	SWP, CVP	Envir., econ.
Federal Energy Regulatory Commission (FERC) licenses (project No.):			
NF Feather river releases (P-1962)	Feather WY forecast	FERC, U.S. Forest Service (USFS), Pacific Gas and Electric	Envir., econ.
Upper American release (P-2101)	American WY forecast	FERC, Sac. MUD	Envir., econ.
SF American release (P-184)	American WY forecast	FERC, El Dorado ID	Envir., econ.
Mokelumne river releases (P-137)	Mokelumne WY forecast	FERC, USFS, Pacific Gas and Electric	Envir., econ.
Lower Mokelumne joint settlement (P-2916)	Mokelumne WY forecast	FERC, East Bay MUD, USFWS, CDFG	Envir., econ.
NF Stanislaus release (P-2019)	Stanislaus AJ forecast	FERC, Utica Power Authority, Northern CA Power Agency	Envir., econ.
MF, SF Stanislaus release (P-2130)	Stanislaus AJ forecast	FERC, USFS, Pacific Gas and Electric/Tri-Dam (pending)	Envir., econ.
SF Stanislaus release (P-1061)	SJ index	FERC, USFS, Pacific Gas and Electric	Envir., econ.
Tuolumne releases (P-2299)	SJ index	FERC, Turlock ID, Modesto ID, H. Hetchy, USFWS, CDFG	Envir., econ.
Merced releases (P-2179)			Envir., econ.
Kaweah river release (P-298)	Kaweah WY forecast	FERC, CDFG, Southern CA Edison	Envir., econ.
Tule river releases (P-1333)	Tule WY forecast	FERC, CDFG, Pacific Gas and Electric	Envir., econ.
Lundy project operation (P-1390)	Mono forecast	FERC, USFWS, BLM, USFS, CDFG, Southern CA Edison	Envir.

TABLE 1. (*Continued*)

| Regulation/project	DWR forecast	Agencies affected	Major concern (Safety/envir./econ.)
Water rights agreements			
Deficiency criteria	Feather AJ forecast	SWP, Joint Water District (WD) Board, Western Canal WD	Econ.
Deficiency criteria	Frenchman, Davis forecast	SWP, Upper Feather Water rights holders	Econ.
Storage cost agreement	Mokelumne WY forecast	East Bay MUD, Northern SJ WCD	Econ.
Kern member allocations	Kern forecast	Northern Kern WSD, Kern Delta WD, Bakersfield, Buena Vista WSD	Econ.
CVP deficiency criteria	Shasta WY forecast	SJ exchange contractors	Econ.
CVP deficiency criteria	Shasta WY forecast	Sacramento river water rights contractors	Econ.
Project water allocations			
SWP deliveries	Sac.–SJ monthly forecasts	SWP, ~20 WA	Econ.
CVP deliveries	Trinity–SJ monthly forecasts	CVP, ~110 WA	Econ.
Kings River service area deliveries	Kings monthly forecasts	Kings River WA	Econ.
Major reservoir operations			
Trinity Lake	Trinity WY forecast	CVP	Safety, envir., econ.
Lake Shasta	Sac. WY forecast	CVP, SWP	Safety, envir., econ.
Lake Oroville	Feather WY forecast	SWP, CVP	Safety, envir., econ.
Bullards Bar Reservoir	Yuba WY forecast	Yuba County WA, SWP, CVP	Safety, envir., econ.
Folsom Lake	American WY forecast	CVP, SWP	Safety, envir., econ.
Camanche and Pardee Reservoirs	Mokelumne WY forecast (secondary)	East Bay MUD	Safety, envir., econ.
New Melones Reservoir	Stanislaus WY forecast	CVP, SWP	Safety, envir., econ.
New Don Pedro Reservoir	Tuolumne WY forecast	Modesto ID, Turlock ID, CVP, SWP	Safety, envir., econ.
Exchequer Reservoir	Merced WY forecast	Merced ID, CVP, SWP	Safety, envir., econ.
Millerton Lake	SJ WY forecast	CVP, SWP	Safety, envir., econ.
Pine Flat Reservoir	Kings WY forecast	USACE, Kings River CD and WA	Safety, envir., econ.
Terminus Reservoir	Kaweah WY forecast	USACE, Kaweah Delta WCD	Safety, envir., econ.
Lake Success	Tule WY forecast	USACE, Tule River Association	Safety, envir., econ.
Lake Isabella	Kern WY forecast	USACE, Kern agencies	Safety, envir., econ.
Lake Tahoe	Tahoe AJ forecast (secondary)	Truckee water master	Safety, envir., econ.
Lake Davis	Grizzly Creek WY forecast	SWP	Envir., econ.
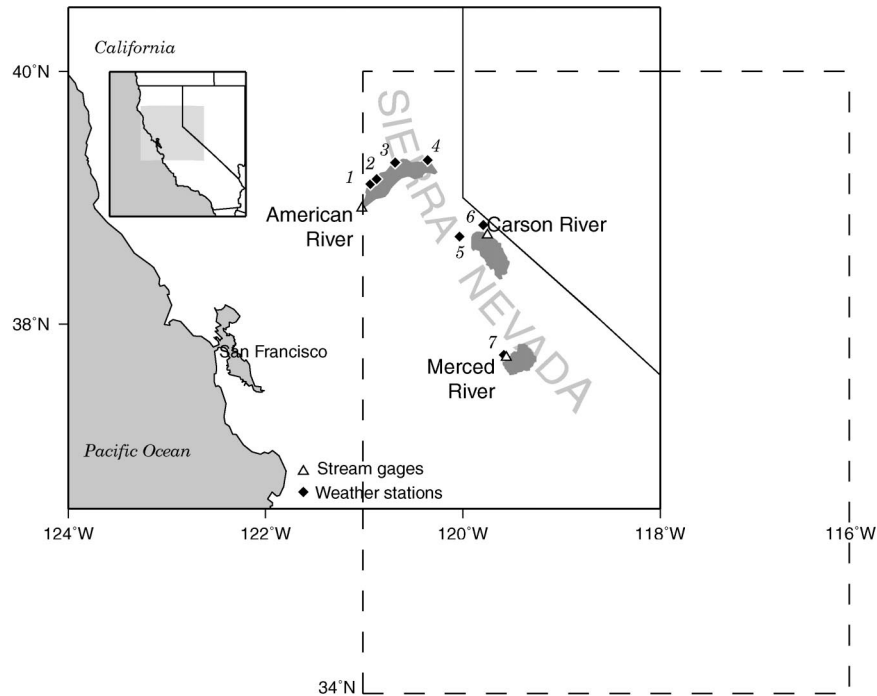
FIG. 1. Overview of the study area. The dashed box defines the geographic region of satellite-based datasets used herein.

have been designed to represent very-finescale variations (order of 30–100 m) of the land surface and the meteorological inputs and have been designed to incorporate more meteorological inputs (e.g., winds and humidities). With the advent of detailed digital elevation models (DEMs) for most terrestrial surfaces, and with the growing number of vegetation and soil representations at similar DEM scales, the primary limiting factors in the application of snowpack and snowmelt models continue to be the lack of spatially resolved meteorological inputs on the same grids as are used to represent the land surface properties and the continuing lack of reliable areal observations of hydrologic and snowpack conditions at comparable scales within the basins.

Current snowpack/snowmelt models are still designed either within the constraints of historical in situ data availability (i.e., often very coarse) or, more recent, for the additional incorporation of meteorological fields that come from (local) weather simulations. The combination of in situ observations and fields that can be estimated (daily or more often) from remote sensing data streams provides opportunities for greater detail and more ground truthing in future simulations than either of these forms of data input.

d. Objectives of this paper

No single observable and parameterizable scale is available at which the complete range of snowpack processes can—in practical terms—be represented quantitatively and, thus, trade-offs will be necessary. Our objectives in this paper are 1) to assess and demonstrate additional spatially and temporally resolved data fields that can be derived from remotely sensed data and 2) to demonstrate the potential value of incorporating these additional data into snowpack/snowmelt models in the Sierra Nevada of California (Fig. 1). We will make the case that, despite the vast range of spatial and temporal scales at work in snowpacks and snowmelt, the appropriate spatial scales lie in some combination of scales that reflects the scale at which snow and insolation can be observed remotely (e.g., Winther and Hall 1999; Simpson and McIntire 2001), the scale to which other meteorological inputs can be interpolated, and (not strictly) the scale at which DEMs describe the terrain. Furthermore, advances in the remote sensing of snow cover and consequent sensing of cloud cover on hourly time scales, summarized herein and described in detail in Simpson and McIntire (2001), now can provide insolation estimates with spatial and, especially, temporal resolutions never before possible. The resulting insolation estimates make possible models with radiative-heating inputs at spatial and temporal resolutions never before feasible over entire basins and ranges. Those models do not yet exist, however, and so our approach will be to demonstrate the sensitivities and improvements possible with examples that use existing, calibrated watershed models of high-altitude parts of the Merced and Carson River basins in the Sierra Nevada of California (Fig. 1). Our findings, with these older models, indicate that a whole new generation of snow-

pack models has become possible and needs to be developed.

2. Data and preprocessing

The newer Geostationary Operational Environmental Satellite (*GOES-8–10*) has four relevant spectral bands: a visible channel (0.55–0.75 μm), a mid-IR channel (3.80–4.00 μm), and two thermal IR channels (10.2–11.2, and 11.5–12.5 μm). At nadir, GOES visible data have 1-km spatial resolution and all IR data have 4-km resolution (Komajda and McKenzie 1994). Full-resolution data were ingested and calibrated to geophysical units using procedures developed by National Oceanic and Atmospheric Administration National Environmental Satellite, Data, and Information Service (Komajda and McKenzie 1994; Planet 1988). The GOES IR data are remapped to the 1-km GOES visible grid using optimal interpolation.

The data are preprocessed to ensure their quality. Valid albedo data lie within the range 0%–100% (Planet 1988). Calibration uncertainties and noise produce a few values (<0.001%) that either exceed 100% or are negative. Simpson and McIntire (2001) describe a remapping procedure that optimizes the dynamic range of the albedo input for snow classification, precluding any possible calibration errors affecting it and preserving the maximum number of pixels for classification.

Histogram filtering is used to remove any outliers in the data (e.g., speckled noise) that can distort the useful dynamic range of the data in any classification (Simpson and McIntire 2001). This filter does not remove gross noise features (e.g., dropouts) in the data; these should be identified and removed separately prior to analysis. Ocean pixels are excluded using a geographic land mask (Simpson 1992).

3. New remotely sensed snowpack/snowmelt-related products

a. Hourly areal extent of snow cover—Brief overview

The high temporal sampling (hourly or faster) of GOES provides about 12 daylight scenes per day at a given midlatitude location. When such data are available, a recurrent neural network designed for clear land, cloud, and snow separation (RNNCCS) improves snow cover/cloud cover/clear land classification skill (Simpson and McIntire 2001). The RNNCCS uses spectral and texture information from the current image in the time series as input, along with textures from the previous texture image input and the classification from the previous network output (Fig. 2). This approach allows the network to have an operational ''short-term memory'' of both texture and classification data from the previous image. By putting previous texture and previous classification information into the current classification, the RNNCCS functions more like a human be-

ing would in solving the classification problem. The RNNCCS combines a short-term memory (data and information from the previous RNNCCS analysis) with a ''long-term memory'' (the RNNCCS's weights and biases) to determine the current classification.

Specifically, the RNNCCS (Fig. 2b) shows that, for image i in the sequence, output data (X, Y, Z) from image $i - 1$ are input to the classification of image i. The homogeneity texture H_{i-1} input for image $i - 1$ is subtracted from the homogeneity texture H_i for image i and is also used as an input for image i. This network in general is more accurate than a single feed-forward neural network because of the information contributed by the short-term memory. If, for example, the previous RNNCCS classification assigned pixel P as snow, and the texture data for pixel P remain close to their previous values, then the RNNCCS knows that pixel P probably still is snow. If, however, a cloud had entered the field of view of pixel P or the snow in pixel P had melted, then the texture for pixel P would also have changed. The feedback loop would alert the RNNCCS that pixel P probably is no longer snow covered. Details of the training set and the method for training a recurrent neural network are given in Simpson and McIntire (2001).

Clouds cast shadows that are especially large under wintertime conditions when the sun is relatively low in the sky (Simpson and Stitt 1998). In addition, mixed pixels often occur at cloud edge boundaries. Some of the properties (spectral and textural) of cloud shadow/cloud edge pixels are similar to those of either snow or some land surfaces, which can lead to classification errors regardless of the classification method used. Postprocessing determines whether a pixel classified as snow was, in fact, a cloud edge/cloud shadow pixel (see Simpson and McIntire 2001), based on generalized cloud shadow detection procedures developed by Simpson and Stitt (1998) and Simpson et al. (2000).

The snow/cloud/land percentage compositions of pixels are determined using a linear mixing model similar to that of Adams et al. (1986). The RNNCCS was trained to identify pure classes (clear land, cloud, or snow) by setting the appropriate output to a value of 1 and all other outputs to 0. If a snow pixel is not pure (i.e., it contains more than one class), then the activation of the snow output node will be less than 1, and the clear land and/or cloud output node will be greater than 0. The linear mixing model is created based on this principle. Using algebra, it can be represented as

$$L_x + L_y + L_z = 1, \qquad (1)$$

where L_x, L_y, and L_z are the percentages of clear land, cloud, and snow for a given pixel. Equation (1) is solved for L_x, L_y, and L_z using the continuous outputs (O_x, O_y, O_z) of the neural network. Details are given in Simpson and McIntire (2001).

Random RNNCCS-based GOES classifications, from throughout the 1999 snow season, were validated with snow sensor data provided by the California Coopera-

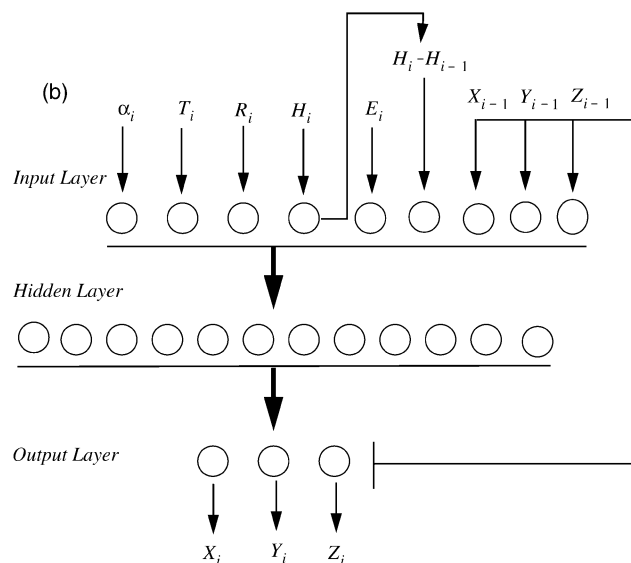## Overview of Neural Network Procedure
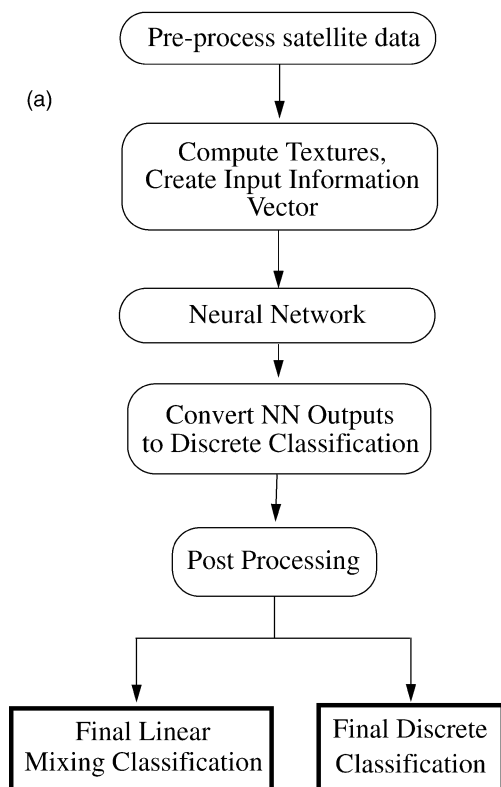
RNNCCS: Feedback

FIG. 2. (a) Overview of the snow/cloud/clear land classifier and (b) the RNNCCS used by the classifier. Inputs are from hourly GOES satellite data: α_i is visible albedo, T_i is 11-μm brightness temperature, R_i is radiance of the 3.9-μm data, H_i is visible-band homogeneity texture measure, E_i is entropy-band texture measure, and $H_i - H_{i-1}$ is the difference between current time step i and previous time step $i - 1$ texture measure; (X_i, Y_i, Z_i) and $(X_{i-1}, Y_{i-1}, Z_{i-1})$ are the current and previous time step neural network output classes (clear land, cloud, snow, respectively). Adapted from Simpson and McIntire (2001).

tive Snow Surveys Program. Total snow/land classification accuracy, based on 1769 GOES–snow sensor pairs, was 97%. Details of the validation procedure, including limitations, are discussed in Simpson and Mc-Intire (2001). A representative example (Fig. 3a) shows the broadband GOES visible albedo data for 19 April 1999 at 1530 local time. The region imaged corresponds to the dashed box in Fig. 1. It contains clear land, ocean, clouds, and snow in the Sierra Nevada (dendric pattern running NW to SE in the center of the image). Both the RNNCCS–linear mixing model classification (Fig. 3b) and the discrete RNNCCS classification (Fig. 3c) identify the basic patterns of clear land, cloud, and snow seen in the visible data (Fig. 3a). Ocean data are excluded from consideration (see Simpson 1992). The locations of snow sensor validation stations are given by either the yellow boxes (RNNCCS classification and snow sensor agree) or the light blue boxes (classifications disagree). Agreement is at the 93% level for this scene.

b. Hourly RNNCCS insolation

Hourly insolation Q reaching the ground was estimated for each pixel (1-km spatial resolution) in a given GOES scene using Lumb's (1964) empirical formula but modified to include a factor $\overline{d}/d$, which accounts for the instantaneous separation d between the earth and the sun:

$$Q = 135(\overline{d}/d)^2 fs, \qquad (2)$$

where $f = a + bs$, a and b are constants dependent on the percent cloud cover in octas, and s is the mean of the solar zenith angles at the beginning and end of a given hour. The accuracy of Lumb's parameterization has been verified by many independent sets of observations (e.g., Simpson and Paulson 1979). The number of octas for a given pixel was determined from the cloud-cover percents in a 5×5 pixel area centered on that pixel using the RNNCCS–linear mixing model classification. The modifying term $(\overline{d}/d)^2$ is recom-
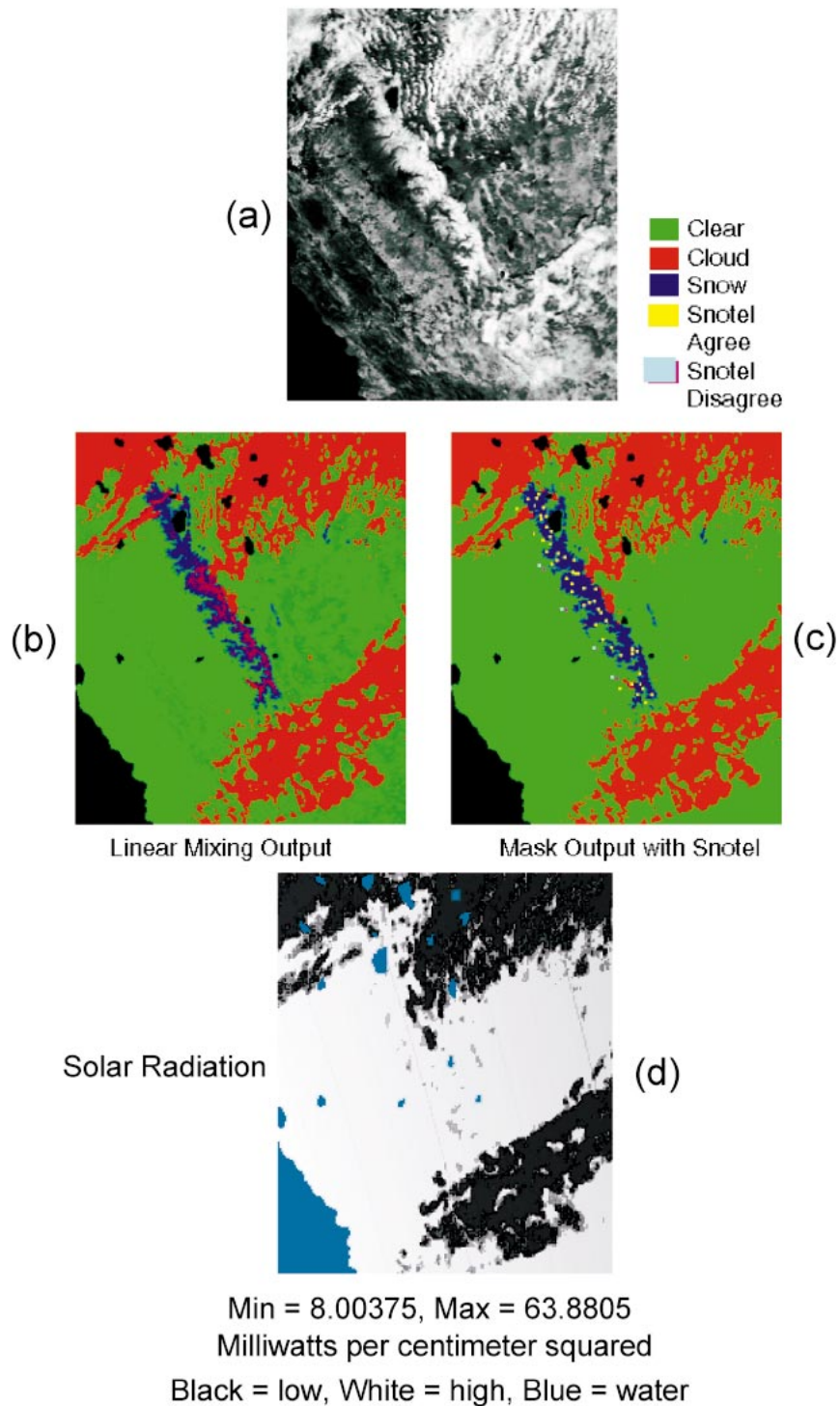
April 19th, 1999, 3:30 pm

FIG. 3. (a) GOES broadband visible data for 19 Apr 1999. The area imaged corresponds to the dashed box in Fig. 1. (b) The RNNCCS–linear mixing model classification. (c) The RNNCCS discrete classification with snowpack telemetry-instrumented validation (SNOTEL) sites shown. (d) Insolation reaching the ground based on satellite-detected cloud cover. See text for details.

TABLE 2. Number of *GOES-10* scenes (500 × 600 pixels) at 1-km spatial resolution that were used in mean monthly statistics for the 1999 period that was studied.

Month	No.	Month	No.
Mar	57	Jul	302
Apr	289	Aug	216
May	207	Sep	260
Jun	241	Oct	6

mended by Sellers (1965), where $\overline{d}$ is the mean earth–sun distance (taken as 1) and d is the instantaneous distance based on yearday j. Daily values of insolation were computed by summing hourly estimates [Eq. (2)] from sunrise to sunset. Results also were compared with Kimball's (1928) empirical estimate of insolation:

$$Q_{day} = Q_0(1 - 0.071C), \qquad (3)$$

where Q_0 is a mean daily value taken from Kimball (1928) and C is cloud cover in tenths. Note that C is computed as described above but in tenths, not in octas. For random dates during the 1999 snow season, Eqs. (2) and (3) estimate insolation to within about ±5% of each other. Figure 3d shows the insolation arriving at the ground for 19 April 1999 based on cloud cover determined from the 1530 LT GOES data. Spatial variation in cloud cover is the primary factor that influences spatial variation in insolation on the hydrologic basin scale. Topographic relief adds a supplemental component of variation to the insolation as compared with that received on a flat plane. Vegetation also affects the insolation reaching the snow (also see section 5).

4. Remote sensing results

a. Daily variability

Cloud cover can significantly reduce the amount of insolation reaching the ground (and hence the energy available for snowmelt) over a broad spectrum of space and time scales. Cloud cover also precludes the detection of snow beneath it if visible–infrared wavelengths are used. Although microwave remote sensing can image through the clouds, its coarse space scale (>25 km, depending on wavelength), coupled with other technical problems (e.g., thin layers of water from snowmelt on the surface interfere with microwave detection techniques; limited temporal sampling at most locations), precludes resolving the underlying snow field on the space and time scales required for accurate basin-scale modeling of snow accumulation and snowmelt. Below, we use daily time series of GOES data for the 1999 snow season (Table 2) to assess the effects of highly variable cloud cover on snow basin hydrological behavior.

b. Basin-scale statistics

The Merced River basin above Yosemite Valley, the Carson River basin above Markleeville, and the American River basin above North Fork Dam (Fig. 4), all in California–Nevada, were selected for detailed analysis. These basins are representative of different types of hydrologic river basins (e.g., high versus low elevation, leeward versus rain shadowed) in the Sierra Nevada drainage. The Merced and Carson River basins are higher-altitude basins (roughly 1500–4000 m) than the American River basin (roughly 200–3000 m). The Carson River drains the eastern rain-shadowed slopes of the Sierra Nevada; the Merced and American Rivers drain the western windward slopes.

Mean monthly cloud cover and its coefficient of variation (mean/standard deviation) for the Merced River basin for April–June of 1999 are shown in Figs. 5a–f. Corresponding data for the Carson River basin are shown in Figs. 5g–l. Table 2 lists the number of GOES scenes in a given month used to compute these cloud-cover statistics. Each of these GOES cloud-cover maps has a spatial resolution of about 1 km^2.

The mean monthly maps show 1) considerable mean monthly variation in cloud cover from month to month, 2) considerable between-basin variation in cloud cover, 3) considerable small-scale (within basin) variation in cloud cover, and 4) large coefficients of variation of cloud cover across a basin and over time.

Analogous data for the entire 1999 snow season (Figs. 6a,c,e) are even more revealing. They show that 1) in general, the lower-altitude parts of a given basin (western edges in the cases of the Merced and American, and eastern edges for the Carson) experience less cloud cover than do the higher-altitude edges, 2) considerable spatial variation in cloud cover exists between these extremes within a given basin, and 3) the cloud patterns are basin specific. Moreover, the corresponding coefficients of cloud-cover variation (Figs. 6b,d,f) show that cloud-cover variations are typically over one-half of the mean everywhere within a given basin. This result reflects the satellite-derived day-to-day and even image-to-image variability in cloud cover seen in 1999 snow-season GOES images. Thus, a seasonal mean (or climatological mean) is not representative of the space and time variability in cloud cover and insolation. These variations in insolation surely must influence the accumulation and melt of snow within a given hydrologic basin during a given snow season.

c. Daily composites

The hourly sampling rate of GOES data, coupled with the accurate and efficient RNNCCS-based classification, allows all data during daylight hours to be processed in near–real time. A 500 × 600 pixel scene (e.g., Fig. 3) takes less than 2 min to process (including extraction, navigation, calibration, classification, and postprocess-
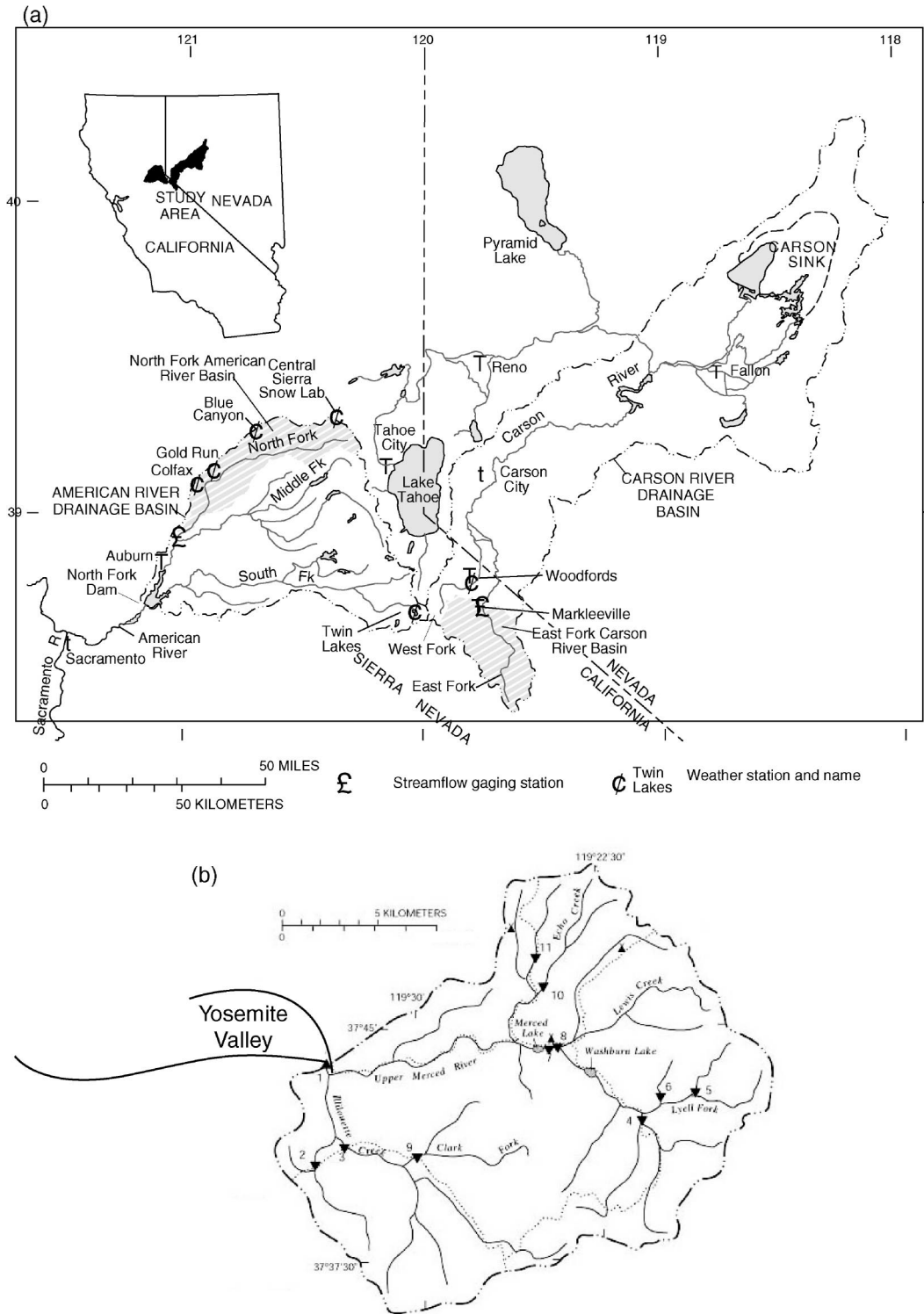
FIG. 4. (a) The East Fork Carson River (above Markleeville, CA) and (b) the Merced River (above Happy Isles Bridge) hydrologic basins.

MERCED RIVER BASIN ABOVE HAPPY ISLES BRIDGE
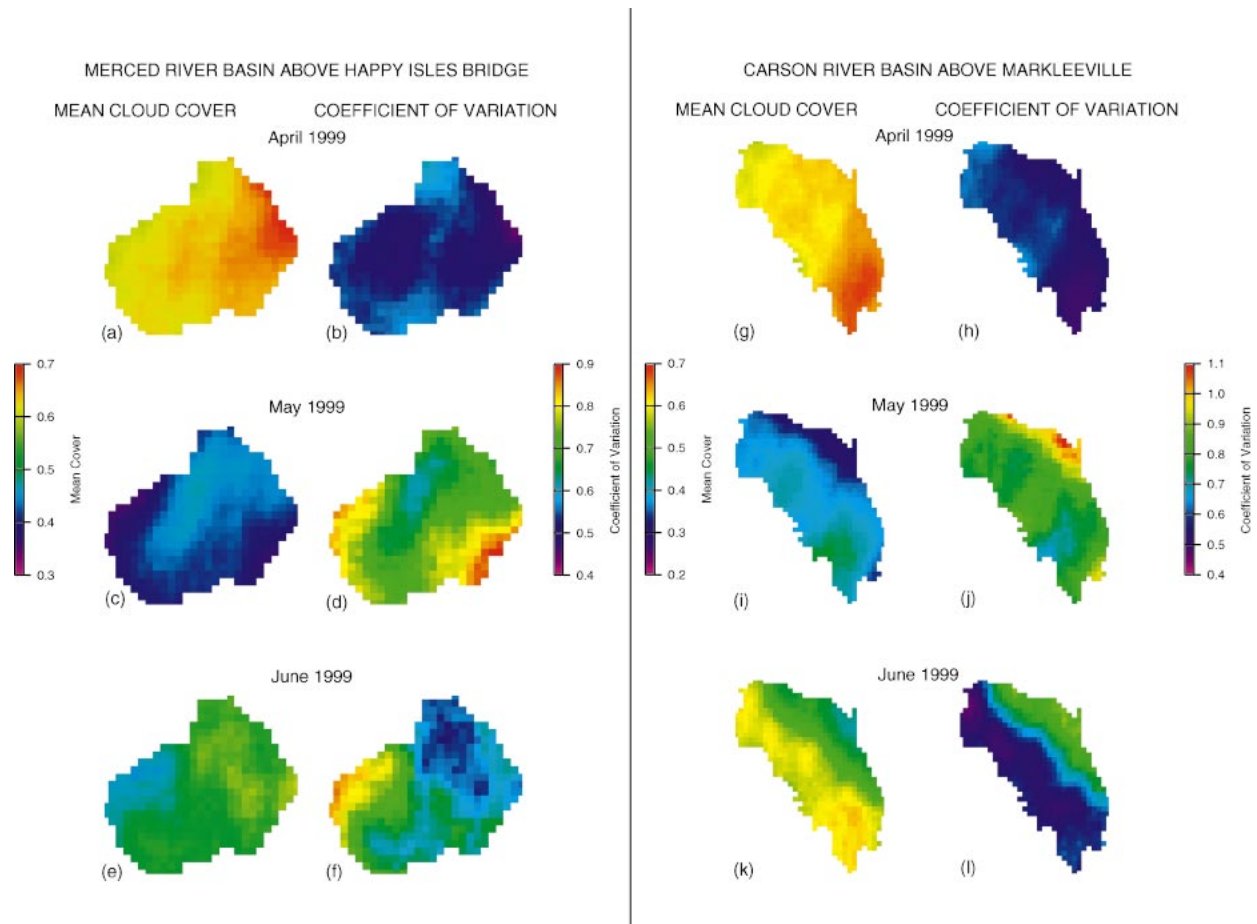
CARSON RIVER BASIN ABOVE MARKLEEVILLE

FIG. 5. Mean monthly cloud cover and coefficient of variation (mean/standard deviation) for the months and basins indicated. See Table 2 and the text for details on data used.

ing). Thus, daily two-dimensional frequency diagrams (Fig. 7), which represent the number of times each pixel was a member of a given class (cloud, snow, or clear land) during a given day, can be computed easily. These frequency diagrams provide useful information that is not contained in the classification of individual scenes, including the following: 1) information on the persistence of snow cover can be obtained from these diagrams, 2) spatial and temporal variability in the cloud field is contained in the composite, and 3) the composite can help to identify significant errors in classification should such errors occur.

5. Cloud-cover issues

a. Clouds and hydrologic basins—Scales of variability

Clouds have a wide variety of shapes and sizes and occur at different levels in the atmosphere [e.g., low (stratus, stratocumulus), middle (altocumulus), and high (cirrus, cirrocumulus, cirrostratus)]. A description of these and other cloud genera/species, as well as their

physical and optical properties, is given by the World Meteorological Organization (1956). Clouds also vary over a broad range of spatial scales, from about 100 m to the planetary scale (20 000 km), with the magnitude of cloud variation increasing with spatial scale (Welch et al. 1988; Séze and Rossow 1991). Most cloud variation, however, occurs on spatial scales greater than 30–50 km (Hughes and Henderson-Sellers 1983). Temporal variation in clouds occurs on diurnal, synoptic, seasonal, and interannual scales (Rossow 1993). Observations of clouds also pose complications and limitations. The view of clouds as seen by a ground-based observer (or instrument), for example, is different from that seen from above by a satellite or aircraft. Moreover, subpixel-scale clouds can elude detection in satellite data.

The hydrologic basin scale is the fundamental structural unit for modeling streamflow derived from snowpack. In the Sierra Nevada watersheds, this basin scale typically is 25–100 km. Different subregions, however, occur within the larger basin scale because of variations in relief across the basin and/or phenological variations in vegetation cover. Thus, there is a significant overlap
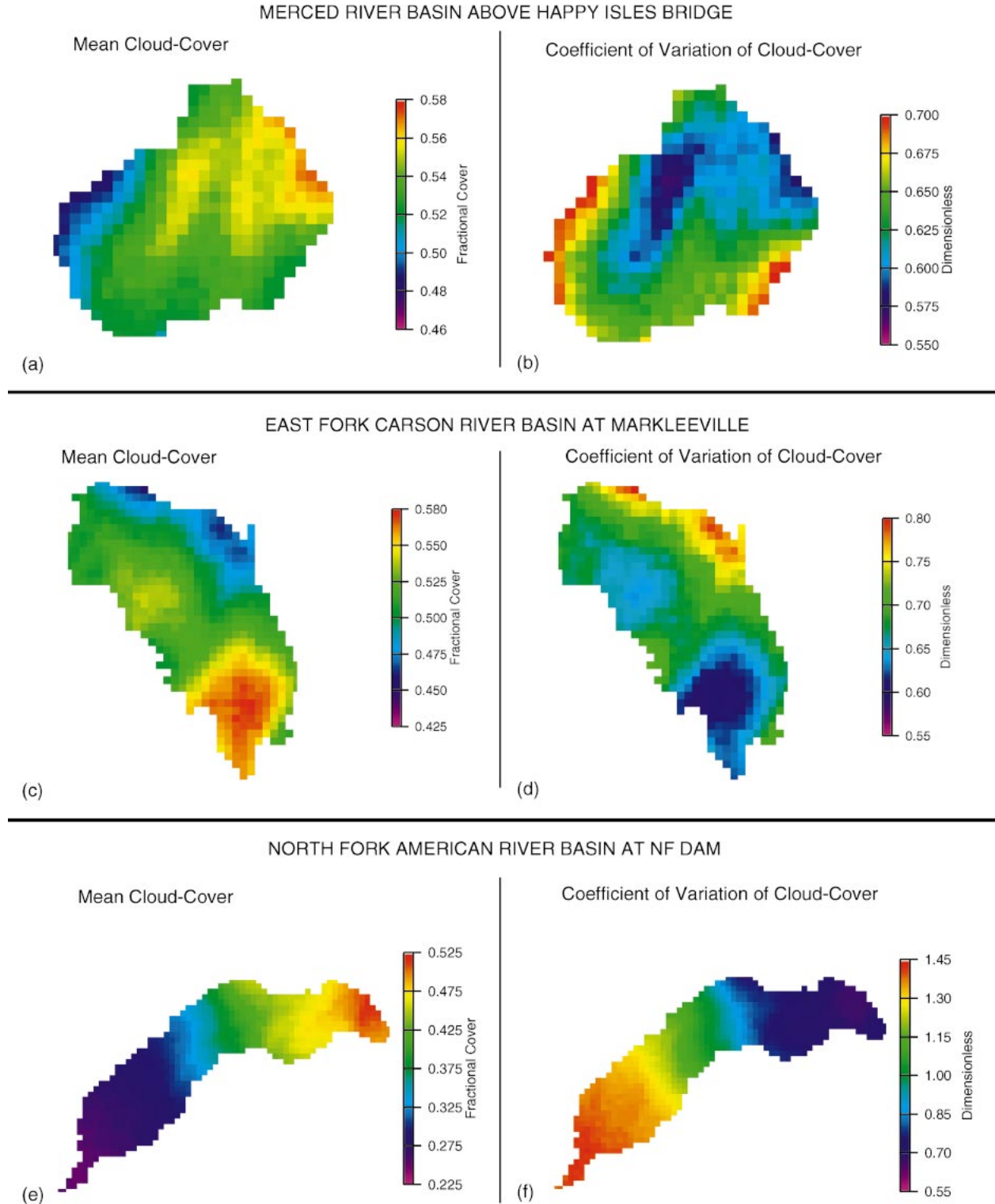
MERCED RIVER BASIN ABOVE HAPPY ISLES BRIDGE

Mean Cloud-Cover

Coefficient of Variation of Cloud-Cover

(a)

(b)

EAST FORK CARSON RIVER BASIN AT MARKLEEVILLE

Mean Cloud-Cover

Coefficient of Variation of Cloud-Cover

(c)

(d)

NORTH FORK AMERICAN RIVER BASIN AT NF DAM

Mean Cloud-Cover

Coefficient of Variation of Cloud-Cover

(e)

(f)

FIG. 6. Analogous to Fig. 5 but for the entire 1999 snowmelt season.

Colors represent the number of times a pixel was
a member of each class (cloud, snow, or clear) during one day

a) Clear

b) Cloud

c) Snow
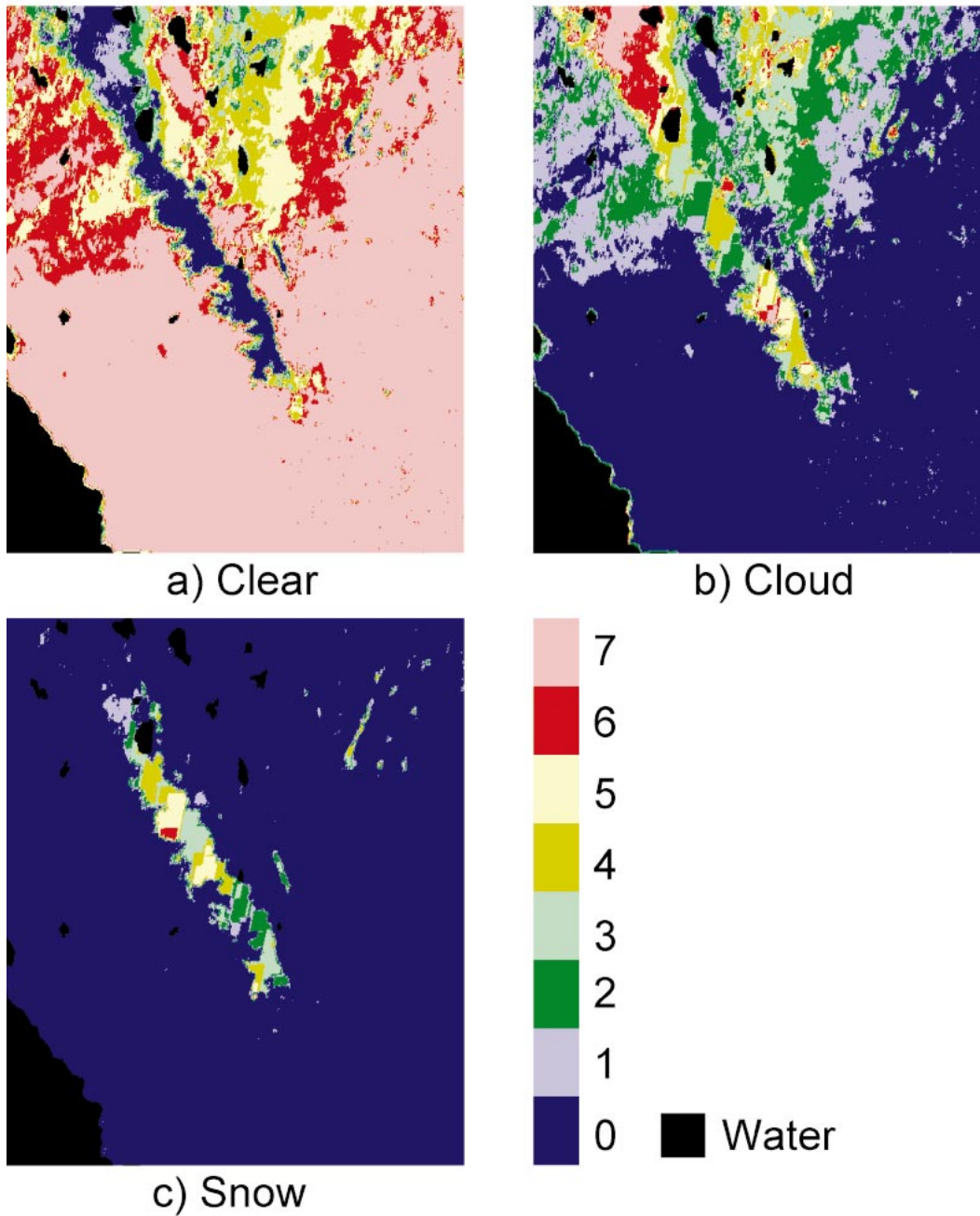
FIG. 7. Two-dimensional frequency diagrams that show the number of times in a day (19 Apr 1999) that a given pixel was a member of a specific class (cloud, snow, or clear land).

between the spatial and temporal scales of variability associated with clouds and those associated with basin hydrological behavior. Accurate modeling of snowpack-derived streamflow requires accurate representation of spatially and temporally varying insolation as a model input.

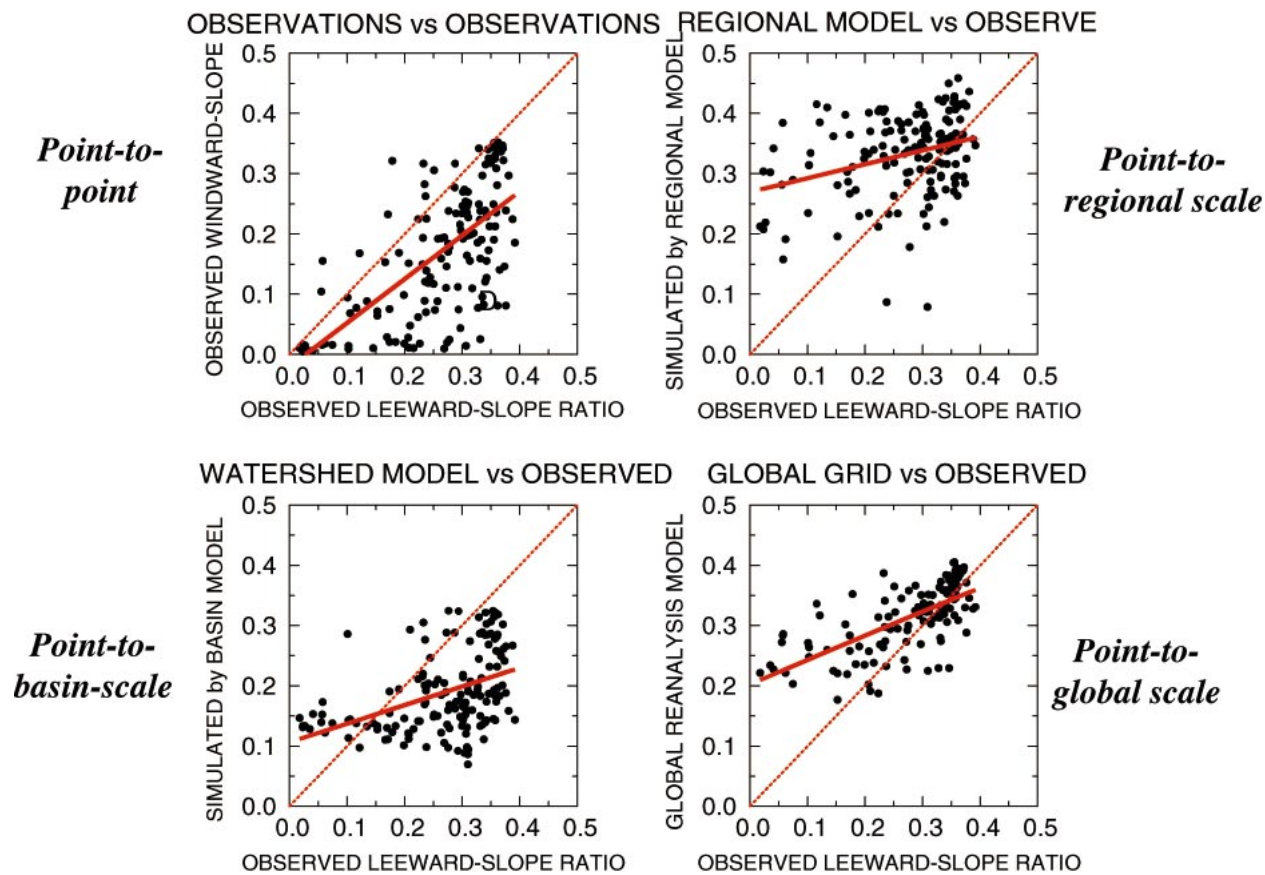Insolation provides the ''fuel'' for melting snow in mountainous regions like the Sierra Nevada (Aguado

FIG. 8. Ratios of daily insolation rates from various sources around the Sierra Nevada to estimates of the corresponding top-of-atmosphere insolation rates. Windward observations are from the Central Sierra Snow Laboratory, leeward observations are from the Sierra Nevada Aquatic Research Laboratory, regional simulated values are from the Regional Spectral Model (Juang et al. 1997; Dettinger et al. 1999) nested in the National Centers for Environmental Prediction–National Center for Atmospheric Research (NCEP–NCAR) reanalysis fields (Kalnay et al. 1996), watershed model values are from a PRMS model of the American River basin (Jeton et al. 1996), and global values are from the NCEP–NCAR reanalysis.

1985). Most basin-scale streamflow models (e.g., PRMS) use either in situ observations of insolation or, more common, infer deviations of insolation from clear-sky values using contrasts between wet and dry days and daily air temperature ranges.

Clear-sky insolation can be calculated precisely based on date, time of day, value of the solar constant, and well-known laws of physics (e.g., Sellers 1965; Sayliegh 1977; Simpson and Paulson 1979). Cloud cover, which varies rapidly in both space and time, complicates both the modeling/parameterization of insolation and the space/time extrapolation of point observations of insolation to the hydrologic basin scale. For example, comparisons of daily deviations of insolation from clear-sky estimates for the Sierra Nevada (Fig. 8) show that 1) point-to-point observations of insolation often have poor correlation from basin to basin, 2) regionally modeled insolation often is poorly correlated with observations, 3) watershed model–inferred insolation (generally based on air temperature) often is poorly correlated with observations of insolation, and 4) global mod-

eled and gridded insolation often is poorly correlated with point observations. In fact, detailed analysis of cloud-cover variability derived from satellite data (Table 2), using the retrieval scheme of Simpson and McIntire (2001) outlined above, shows significant temporal variability in cloud cover (and thus insolation) on an hourly time scale for the Merced, Carson, and American River basins (Fig. 9) during the 1999 study period. Moreover, there is considerable spatial variation in cloud cover and insolation for these three Sierra Nevada river basins during the same period. Indeed, all three basins are partially cloud covered about 45% of the time (Fig. 10).

Highly variable and unpredictable cloud cover confounds model-based parameterization of insolation and its extrapolation from point observations of cloud cover to the hydrologic basin scale. We assert that significant parts of the rms error that occurs between modeled and observed estimates of streamflow is associated with errors in the insolation estimates used as inputs to the hydrologic models. Hourly estimates of insolation, based on GOES satellite data at 1-km spatial resolution

Merced River Basin

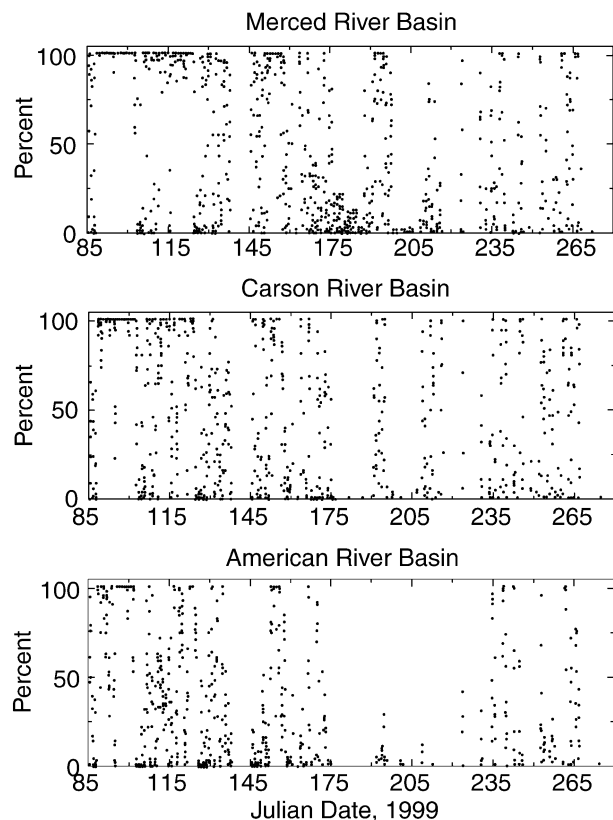## Carson River Basin

American River Basin

Julian Date, 1999

FIG. 9. Hourly retrievals of percent cloud cover derived from GOES data using the GOES-based retrieval scheme of Simpson and McIntire (2001) for three Sierra Nevada basins.

FIG. 10. Analogous to Fig. 9 but for percentage of a given Sierra Nevada river basin area covered by cloud (spring/summer 1999).

(Fig. 3), provide a means to improve significantly the insolation inputs to, and thereby streamflow outputs from, these models.

Average (clear sky) insolation can be computed on a pixel basis using a radiative transfer model (RTM). Such an approach has a physical, as opposed to a statistical [Eqs. (2) or (3)], basis. A time-varying RTM that accounts for clouds and snow is impractical for the intended application, however, for the following reasons: 1) the various input data required to initialize an RTM generally are not available for an arbitrary location and are not available in real time; 2) departures between a best-guess estimate of required atmospheric properties (e.g., aerosol distribution or vertical profiles of temperature and humidity) that might be used to initialize an RTM and those of the actual atmosphere above a given location at a given time often are large, introducing a significant error in to the RTM calculation; 3) surface reflectance properties, also required by the RTM, are largely unknown and vary spatially and temporally (e.g., phenology, wet versus dry surface); and 4) the required execution time for a pixel-based RTM computation over a relatively large area is inconsistent with the real-time/high-spatial-resolution requirements of the intended application.
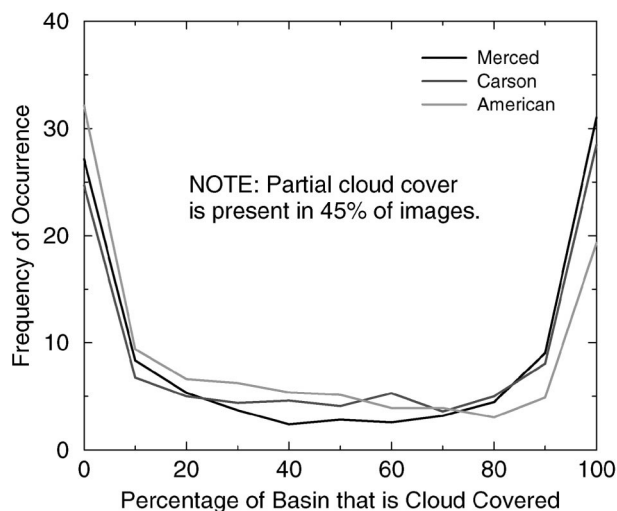
b. Accommodating cloud-cover variations in two existing models of snowmelt runoff

An example of a hydrologic model with spatially distributed parameterizations of daily snowpack heat and water budgets is PRMS (Leavesley et al. 1983). The spatial variability of land characteristics that affect snowpack and runoff generation is represented in PRMS by hydrologic response units (HRUs), within which runoff responses to precipitation or snowmelt inputs are assumed to be homogeneous. HRUs are characterized and delineated in terms of physiographic properties that determine hydrologic responses: elevation, slope, aspect, vegetation, soils, geology, and climate. In the models used here, HRUs were designed to incorporate all cells, on 100-m grids, that share nearly identical combinations of these physiographic properties, regardless of whether the cells in an HRU form a contiguous polygon [as indicated by the map in Fig. 11a; see also Jeton and Smith (1993)]. The resulting "pixelated" model delineations represent the Carson and Merced River basins in the Sierra Nevada (Figs. 1 and 4) in terms of 50 and 64 HRUs, respectively.

Within each HRU, the heat and water budget responses to daily inputs of precipitation and daily fluctuations of air temperature are simulated. The general structure of PRMS, and its spatial layout for the Merced River model, are shown in Fig. 11. Precipitation is generally (but not necessarily) distributed to model HRUs based on the elevation of the HRU, the observed precipitation at a specified weather station, and historical average relations between precipitation amounts and elevation in the model vicinity. The daily mixes of rain and snow are estimated from each day's temperatures by interpolations between the temperatures at which precipitation historically has been either all rain or all snow (Willen et al. 1971). Interception losses, sublimation, and evapotranspiration
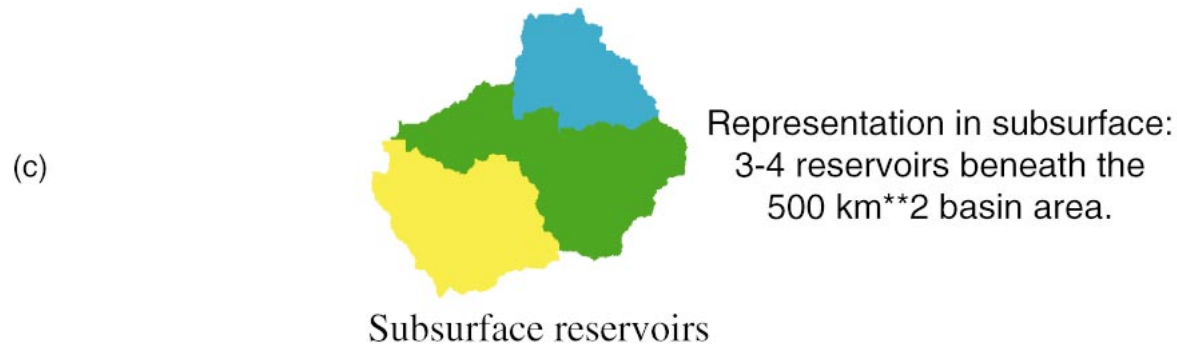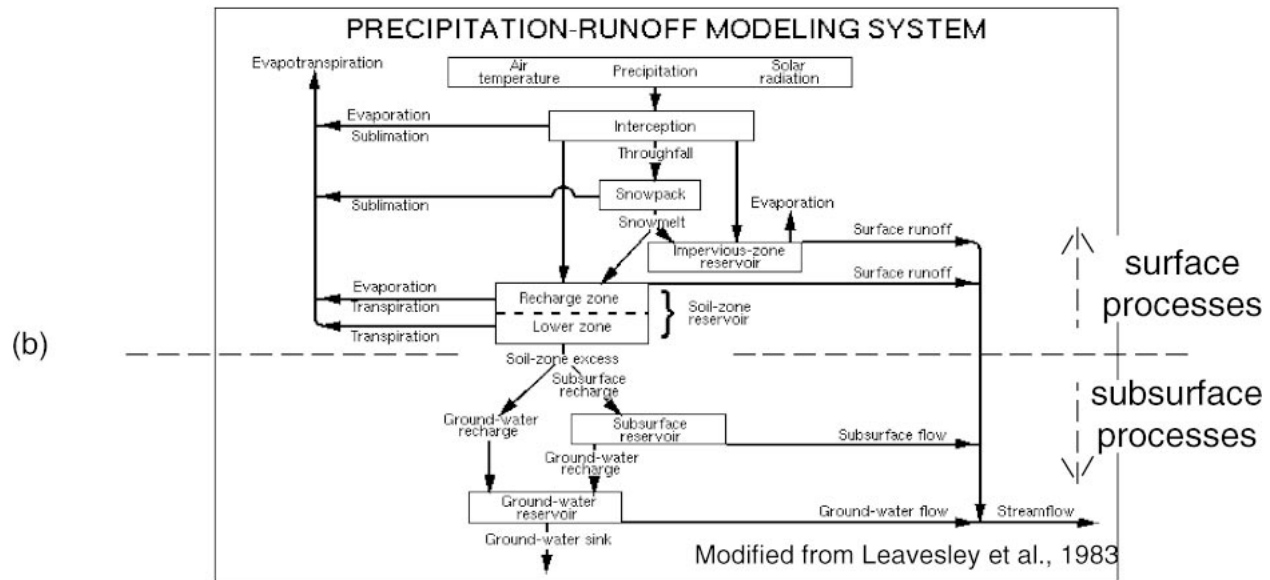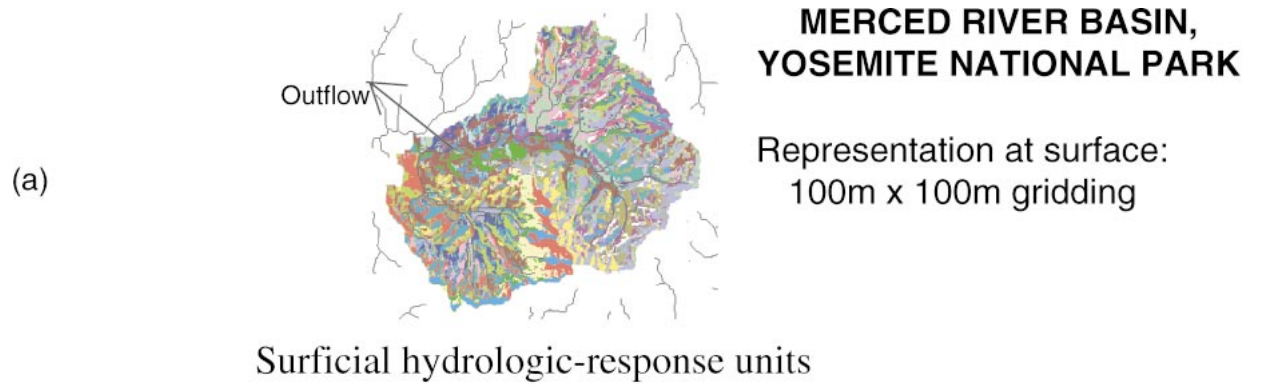
FIG. 11. The U.S. Geological Survey's PRMS, with details for the Merced River model.

are also parameterized and simulated in terms of precipitation and daily maximum and minimum temperatures. Snowpack accumulation, evolution, melt, and, ultimately, the heat and water balances of the snowmelt periods are simulated from the daily inputs of precipitation and daily air temperatures [using the parameterizations of Obled and Rosse (1977)]. Runoff is partitioned between surface runoff, shallow subsurface runoff, deep subsurface runoff, and deep groundwater recharge on the basis of the simulated accumulations of soil moisture at each HRU and of water in deeper subsurface reservoirs that underlie multiple HRUs.

In the absence of observations of daily insolation (as in the calibrated versions of the Merced and Carson River models), either it is estimated from the latitude, day of year, and the presence of clouds as inferred from daily temperatures and precipitation, or it can be input directly if daily observations are available. On days with precipitation, insolation is reduced uniformly over the entire basin, according to a user-specified fraction of clear-sky radiation for that day of year, with separate fractions specified for winter and summer precipitation. Otherwise, small corrections to the daily uniform insolation are made that depend on the maximum daily temperatures, assuming that cloud-shaded days will generally be cooler. If basin-average daily insolation estimates are available, they can be input directly to the model.

The runoff models used here simulate daily stream-flow from about 700 km^2 of the Carson River basin and 500 km^2 of the Merced. Both rivers are mostly free from human influences such as dams, diversions, and major land use changes (Dettinger et al. 2004). The Carson River drains the rain-shadowed eastern slope of the Sierra Nevada, whereas the Merced River drains the wetter, western slopes (Fig. 1). The average elevation of the modeled Carson River basin is 2400 m (with outlet at 1650 m and ridgeline at 3400 m), and that of the Merced River is 2800 m (with outlet at 1200 m and ridgeline near 3900 m). The Carson and Merced Rivers are dominated by springtime snowmelt runoff. Both basins are geologically dominated by the granodiorites of the central Sierra Nevada, with varying additions from volcanic and metamorphic rocks.

The Carson River model is described in detail by Jeton et al. (1996) and has been used to simulate historical streamflows from 1969 to 2001. The Merced River model was designed to simulate daily flows for the period from 1916 to the present (e.g., Dettinger et al. 1998). Indications of the goodness of fit of these models are presented by Jeton et al. (1996) and, more recently, by Wilby and Dettinger (2000) and Dettinger et al. (2004). For both models, overall fits are satisfactory. Goodness-of-fit statistics improve as longer time scales (e.g., monthly and annual totals) are considered, but, in the present context, dailies are most pertinent. From 1950 to 2000, the Merced River model captures 77% of the observed daily flow variability, and the Carson River model captured 82%; rms error statistics for the spring of 1999 are discussed below.

The RNNCCS cloud-cover estimates from the spring of 1999 describe spatial variations in cloud cover (e.g., Fig. 5) and thus insolation over the Merced and Carson River basins. The 1999 seasonal average cloud cover over the Merced River basin (Fig. 6a) is a minimum over the western edge of the basin, near the outlet to Yosemite Valley at about 1500 m above sea level and the westernmost ridgeline of the basin at about 2000 m. The maximum cloud cover was observed at about 4000 m along the ridgeline of the Sierra Nevada on its north-east edge. The basin is partially divided into western and eastern halves by the Clark Range, which extends northward from the center of the southern edge to a point near the center of the basin, and another cloud-cover maximum appears to hug this range's northwestern edge. These season-long mean values, however, arise in the midst of considerable day-to-day and, indeed, image-to-image variability (Figs. 6b and 9). A mirror-image mean structure and similar amounts of spatial and temporal variability are found for the Carson River basin (Figs. 6c, 6d, and 9).

These GOES-based RNNCCS insolation estimates (and other resources like them), thus, permit modifications to the solar radiation inputs to PRMS. At present, however, the RNNCCS insolation estimates provide much more temporally and spatially detailed information than the PRMS models were designed to accommodate. In PRMS, a daily basin-average insolation rate (whether model estimated or input from observations) is assumed to fall uniformly over the basin, above the land surface and plant canopies. The insolation rate reaching the land (or snow) surface of each HRU is then adjusted locally for the influences of the slope and aspect of land surfaces and the density of vegetation canopies that shade the surfaces. Slopes, aspects, and canopy cover are specified for each HRU in a given basin's model. Thus, although PRMS is designed to accommodate simple topographic and (some) surficial influences on HRU-scale insolation, it does not accept spatial variations of the insolation inputs like those induced by cloud-cover variations shorter than a day or smaller than the basin. The influence of spatially varying cloud cover, in particular, cannot be directly accommodated by the current model.

Streamflow simulations of the 1999 snowmelt season using the PRMS insolation estimates (the ''simulations with PRMS insolation'') are compared here with simulations that use RNNCCS daily estimates of basin-averaged insolation (''simulations with basin-averaged RNNCCS insolation'') as inputs in the next section. These latter simulations test the effects of using better, basin-averaged daily insolation rates in the models.

Because the RNNCCS radiation products display clear and important spatial insolation variations within Sierra Nevada basins, the sensitivity of the models to the observed (mean) spatial variations of insolation were tested. Because PRMS is not structured to accept spatially varying insolation inputs, however, the standard estimation of HRU-scale insolation rates used in PRMS had to be circumvented for the test. Because of the large amount of temporal and spatial cloud-cover variation measured by the RNNCCS satellite products and the resulting large variations of insolation within the basins, the models ideally would have been modified to ingest daily, HRU-scale insolation variations, reflecting each day's particular cloud-cover pattern. That level of modification of the well-recognized PRMS code, however, would raise questions of method and is beyond the needs

of the current demonstration. Instead, a model parameter—not intended for this use—was adjusted to approximate the effect of observed spatial variations of insolation in the snowmelt procedures of the model.

The application of these spatially varying insolation inputs in PRMS was not particularly successful, for reasons to be speculated over later, and thus a brief description of the modifications should suffice: in its representation of HRU-scale variations in insolation at the snow surface, PRMS corrects the daily basin-average insolation rate for the vegetation canopy cover over each HRU. In a fortuitous way, a canopy cover parameter, the transmission coefficient for shortwave radiation through the winter vegetation canopy, rad_trcf, is specified for shading of snowpack, separately from all other canopy shading and interception effects. The rad_trcf parameter describes the fraction of downward insolation that reaches the snowpack at each HRU and is only used in the calculations of snowpack heat balances and melting. Thus, adjustments were made to each HRU's rad_trcf parameter to reduce effectively the insolation on snowpacks in some HRUs where cloud cover is more common and to enhance (relatively) the insolation where cloud cover is less common.

This adjustment corresponds to the cloud modifications to insolation at HRU scale without having to modify PRMS to read in separate insolation rates for each HRU. In a complete representation, adjustments would vary through time according to each day's RNNCCS estimates of cloud-cover changes; for this demonstration, however, we adjust only for the 1999 seasonal- and monthly-mean cloud covers (Figs. 6 and 5, respectively). These simulations will be called "simulations with seasonal-average RNNCCS insolation pattern" and "simulations with monthly-average RNNCCS insolation pattern," respectively; these simulations test the value of including spatially varying cloud-cover effects in the current models. When these relatively long-term average cloud-cover patterns are used, the modifications of rad_trcf are small (as illustrated in Fig. 12), and thus the modifications to the insolation reaching the snowpack are small also. The adjustments to Merced River rad_trcf were largest in the high-altitude zones (where vegetation canopy is sparse so that the unadjusted rad_trcf values were large). Cloud-cover values in these zones were largest during the spring of 1999, and insolation was lowest, so that rad_trcf values were adjusted downward to reduce the insolation on the snow. At lower elevations, cloud cover was less common (relative to the basin average), and rad_trcf values were adjusted upward to allow more (than basin average) insolation to reach the snow.

c. Resulting simulations of the spring of 1999

The streamflow simulations with PRMS insolation compare favorably overall to the observed spring 1999 streamflow variations in the Merced and Carson Rivers,
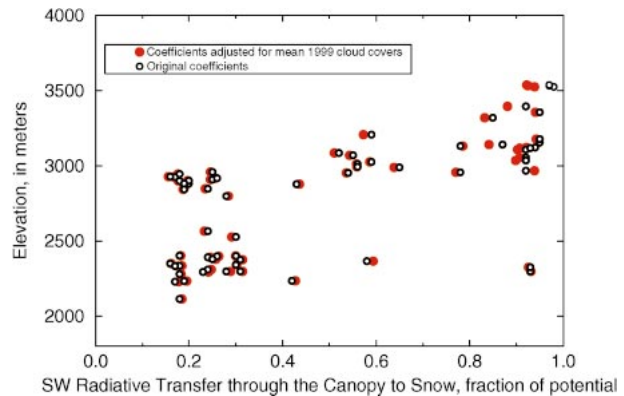

FIG. 12. Relations of shortwave radiative (through plant canopy to snowpack) transfer coefficients to elevation, in the Merced River model (above Happy Isles Bridge), before and after adjustments for seasonal-mean cloud cover, spring 1999.

but with some unrealistic snowmelt and streamflow surges and some missing surges in the simulations. In the Merced River, these false snowmelt events result from poorly inferred insolation variations, as will be shown immediately. The PRMS daily estimates of insolation for the Merced River basin are shown as a red curve in Fig. 13a. Aside from some brief reduction in insolation associated with late-season storms, in the first week of April and near the beginning of May and June, PRMS insolation varies only in a gradual seasonal increase through most of the April–July period. Insolation variations inferred from temperature fluctuations are clearly small in this model. Similar small nonseasonal insolation variations were inferred by PRMS in the Carson River model from the precipitation and temperatures observed at the weather stations used to force that model (Fig. 14a).

Observed and simulated (with PRMS insolation) streamflows are shown as circles and a red curve in Fig. 13b, respectively. After initial low wintertime flows, the simulation with PRMS insolation yields a set of minor snowmelt pulses (and streamflow surges) in late April, earliest May, and mid-May, followed eventually by a major snowmelt in the second half of May. Snowmelt and streamflow decline through June. Observed flows, in contrast, did not surge as much as simulated in late April and earliest May. The observed late May streamflow maximum was smaller than in the simulation and is partially compensated by another later sustained streamflow peak in mid-June. The incorrectly simulated early snowmelt peak in this simulation occurs during the late April period when temperatures had risen enough to poise the snowpack near the melting point and when the PRMS insolation rates are dramatically higher than those calculated from the RNNCCS radiation products (shown by the green curve in Fig. 13a). The PRMS overestimates of insolation in late April fueled the unrealistic early snowmelt pulse. Furthermore, when the model simulates snowmelt events too early in
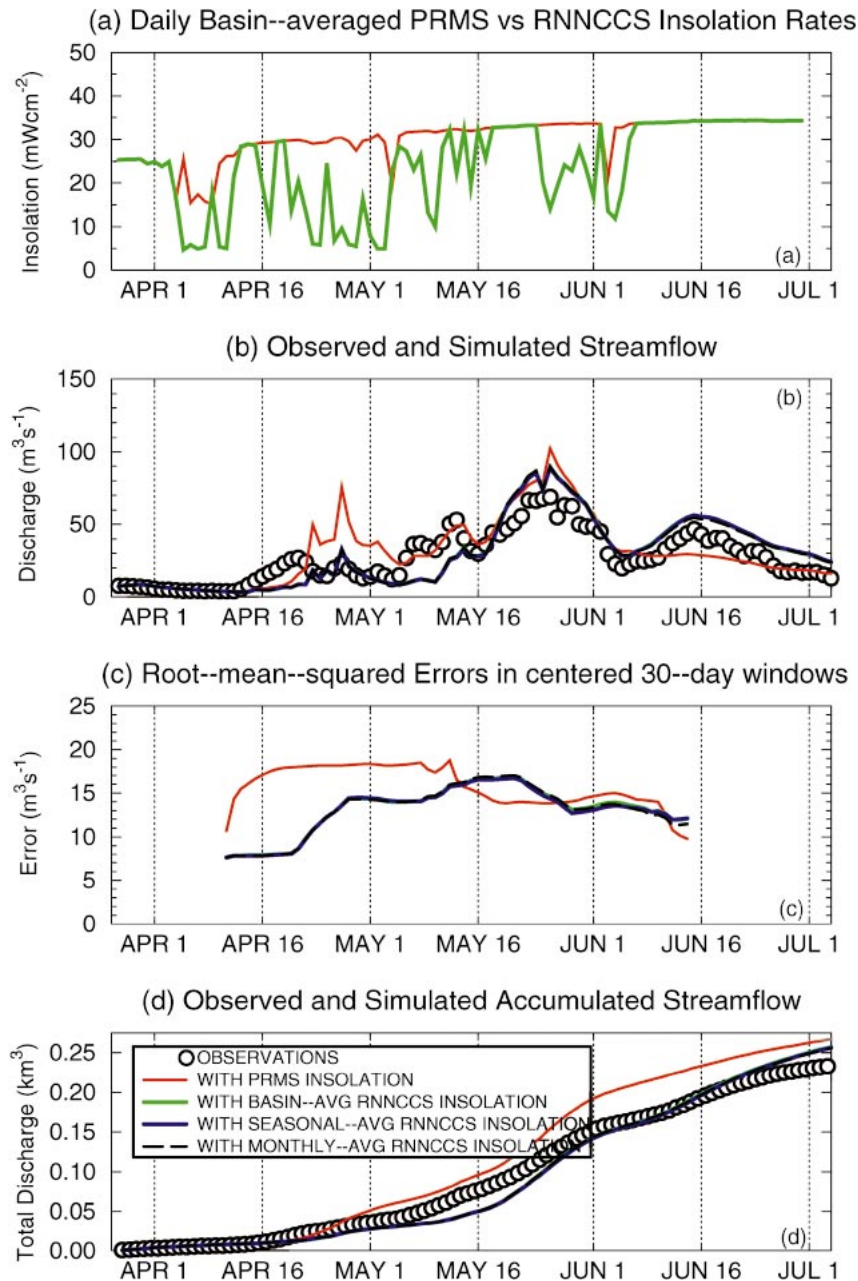
FIG. 13. Comparisons of (a) daily PRMS-estimated and RNNCCS insolation estimates and (b) observed and simulated streamflows, along with (c) rms errors, for Merced River basin at Happy Isles Bridge for the spring snowmelt season 1999. (d) Cumulative volume flow for the different insolation estimates as indicated.

a given year (as in this example), the water that is prematurely released by the model is not available for release and runoff later in the simulation. Thus, to a large exent, the prematurely simulated late April snowmelt pulse also resulted in the missing mid-June snowmelt pulse (and streamflow peak). The corresponding observed and simulated flows in the Carson River are shown in Fig. 14b, which yields much the same story, except that the Carson River model underestimates, rath-

er than overestimates, the peak flows observed during late May and mid-June.

The rms errors, in centered 30-day windows, computed from a comparison of the observed and simulated (obtained using PRMS insolation) streamflows in the two rivers are shown by the red curves in Figs. 13c and 14c. In the Merced River, early in the spring, the premature snowmelt pulse of late April results in relatively large rms errors; by mid-May, the rms errors have de-
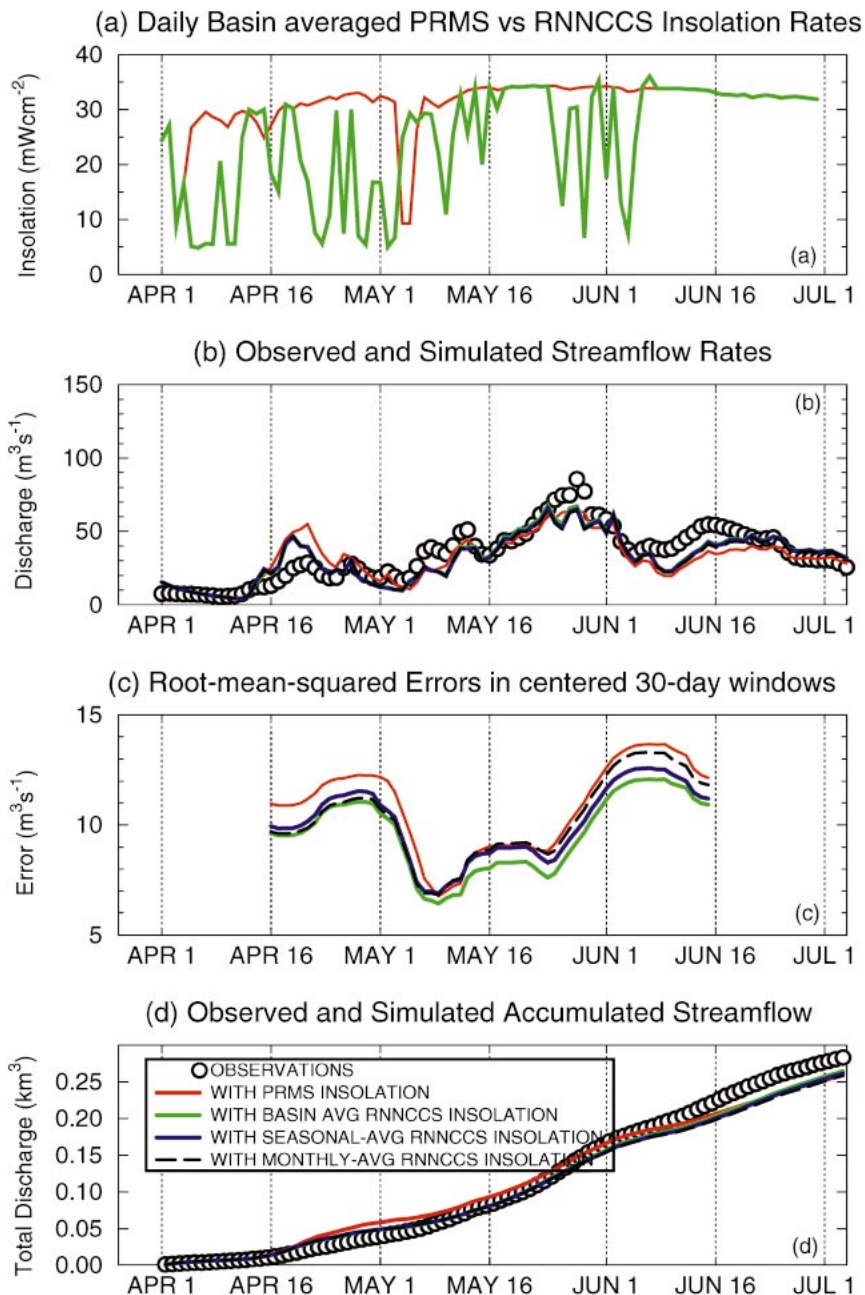
FIG. 14. Same as in Fig. 13 but for the East Fork of the Carson River basin.

clined. In the Carson River, errors are largest both early in the simulations and again at the season's end.

The daily basin-averaged RNNCCS insolation rates for the spring of 1999 are considerably more variable, with many more low-insolation days, than are the insolation rates inferred by PRMS from the daily precipitation and temperature inputs (green curves in Figs. 13a and 14a). RNNCCS insolation rates in April and early May of 1999 and again around the beginning of June are notably lower than are the PRMS values, reflecting many cloud-covered, but not precipitating, days.

On a relatively few days, mostly later in the spring, RNNCCS insolation rates are estimated to be slightly higher than the PRMS-inferred rates, but these deviations are small and probably do not play a major role in the simulated daily snowmelt and runoff rates. Of note, the reductions of insolation to the rain-shadowed Carson River basin by cloud cover, indicated by the RNNCCS estimates, resulted in even greater overestimates of insolation by PRMS during cloudy but nonprecipitating days (Fig. 14a) than in the windward Merced River basin.

Using the RNNCCS insolation rates, the simulation with basin-averaged RNNCCS insolation inputs (green curve in Figure 13b) does not yield the erroneous late April snowmelt pulse that was present in the Merced River simulation with PRMS insolation (red curve in Fig. 13b). Note that the blue curve generally overlies the green curve in Fig. 13b so that the green curve is difficult to see. As a result, also, the simulation with basin-averaged insolation more correctly captures the snowmelt peak in mid-June that the simulation with PRMS insolation missed. Simulated flows during mid- to late May are still oversimulated, however, but not quite as much as in the simulation with PRMS insolation. Overall, in the first half of the spring of 1999, the simulation errors are notably smaller in the simulation with basin-averaged RNNCCS insolation (green curve, Fig. 13c) than in the simulation with PRMS insolation (red curve). In the second half of the season, the simulation with basin-averaged insolation inputs yields rms errors that are not much different from those from the simulation with PRMS insolation. The inclusion of RNNCCS insolation changes in the Carson River simulations yields reductions, relative to the simulation with PRMS insolation, throughout the simulation period (Fig. 14c). In all Carson River simulations, rms errors were highest during the early falsely simulated snowmelt peak and during the late snowmelt peak that was missed in the simulations.

Reservoir managers will often be more attuned to differences in the accumulating total outflows from river basins than to their day-to-day fluctuations. The accumulations of streamflow from the two rivers, in observations and in simulations, are shown in Figs. 13d and 14d. Early in the season, the observations and simulations compare well. By mid-May, the simulation with PRMS insolation overestimates the accumulated flows in both rivers. The simulation with basin-averaged RNNCCS insolation lags behind the observations in the Merced River but, by June, is in excellent agreement with observations, whereas the simulation with PRMS insolation never recovers. By mid-May, the simulation with RNNCCS basin-averaged insolation is in excellent agreement with observations on the Carson, and, by end of season, both simulations have slightly underestimated the observed accumulation.

Using the same daily basin-averaged RNNCCS insolation rates (green curve in Figs. 13a and 14a) but with the seasonal-average RNNCCS cloud-cover pattern accommodated by adjustments to rad_trcf, the simulations with the seasonal-mean RNNCCS insolation pattern yield the streamflow variations shown by the blue curves in Figs. 13b and 14b. These simulations track the simulation with uniform basin-averaged insolation inputs closely throughout the 1999 season. In a similar way, when monthly adjustments are made (dashed black curves), the results are very similar to the simulations with uniform basin-averaged insolation inputs. The effects of adjusting the spatial patterns of insolation are

TABLE 3. Root-mean-square errors ($m^3 s^{-1}$) from four simulations of discharge of the Merced and Carson Rivers during Apr–Jun 1999 and from three simulations during Jun 1998. Simulations are described in the text.

Simulations	Merced River	Carson River
	Spring 1999	
Simulation with PRMS radiation	15.8	10.8
Simulations with basin-averaged RNNCCS insolation	13.1	9.6
Simulation with seasonal-averaged RNNCCS insolation	13.0	10.1
Simulation with monthly-averaged RNNCCS insolation	13.1	10.3
	Spring 1998	
Simulation with PRMS radiation	23.9	8.9
Simulation with basin-averaged RNNCCS insolation	21.5	11.3
Simulation with basin-averaged RNNCCS insolation and RNNCCS snow cover corrections to initial conditions	22.3	5.5

somewhat larger in the Carson River simulations (Figs. 14b,c). It is evident that the relatively rapid cloud-cover changes and attendant insolation variations within the basins (Fig. 9) are not well represented by seasonal or monthly spatial averages, and the current models were not improved by these additional inputs.

The overall April–June 1999 average rms errors for the four Merced and Carson River simulations are shown in Table 3. By this measure, the simulations with basin-averaged insolation inputs in the Merced and Carson River models perform about 21% and 12% better than the simulation with PRMS insolation, respectively. No additional improvements were realized by the simulations with temporally and spatially varying insolation with these models. Thus, as noted previously, the rapid variations of cloud cover and insolation, indicated by Fig. 9, were not represented well by either seasonal or monthly averages. Real improvements may require models that are capable of incorporating insolation patterns that vary according to observations on daily time scales and spatially within a basin.

RNNCCS cloud- and snow cover classifications were also generated during a brief period in June of 1998 and provide another example of the usefulness of RNNCCS insolation (and snow cover) estimates in the Merced and Carson River models. Insolation rates from the PRMS parameterization and from the basin-averaged RNNCCS estimates are compared in Figs. 15a and 15c and show the same unresponsive PRMS insolation variations as were found in the spring 1999 examples. The June 1998 period was one of general and largely featureless snowmelt and streamflow declines and, thus, is not as good of a test of the RNNCCS inputs as was the longer, more varied 1999 interval. Simulated spring 1998 streamflows in the Merced River (Fig. 15b) using the two insolation inputs are generally similar, although with

(a) Daily Basin-Averaged PRMS vs RNNCCS Insolation, Merced basin

(b) Observed and Simulated Merced River Streamflow

(c) Daily Basin-Averaged PRMS vs RNNCCS Insolation, Carson basin

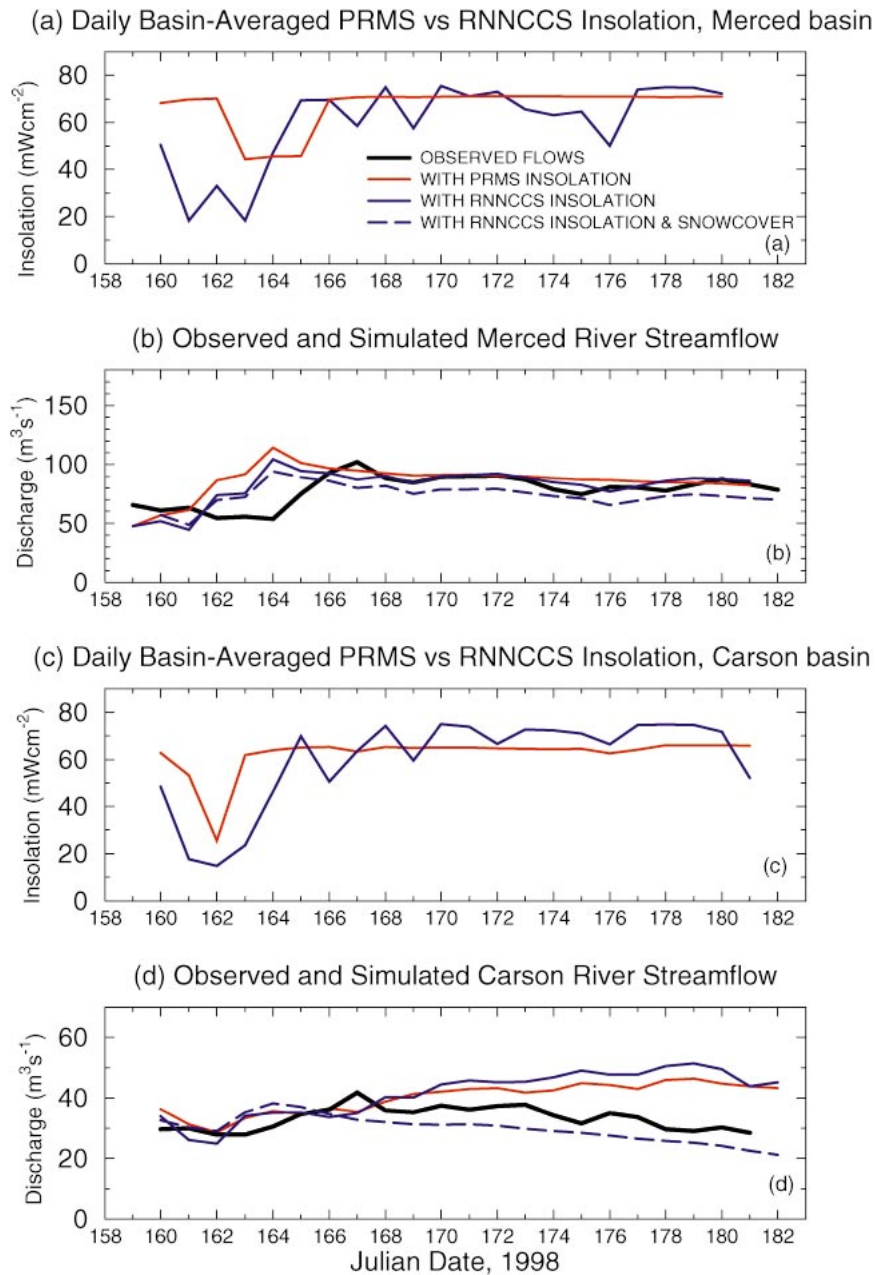## (d) Observed and Simulated Carson River Streamflow

FIG. 15. Similar to Figs. 13a and 13b but for simulations of streamflow in the Merced and Carson Rivers during a part of Jun 1998. See the text for details.

significant improvements in the simulation with basin-averaged RNNCCS insolation inputs (relative to the simulation with PRMS insolation) from days 169 through 177, in response to greater, unrealistically constant insolation rates in the PRMS parameterization during this period. The overall rms error of the Merced River simulations (Table 3) indicates an 11% reduction in error with the RNNCCS insolation inputs. In the Carson River, both simulations yielded unrealistically large flows throughout the second half of the simulation period. (Fig. 15d). This overestimation was resistant to

various attempts at revisions to the input series and, eventually, was ascribed to an overestimation of the overall amount of snow in the initial conditions for these simulations; this hypothesis is explored in the next section.

The current PRMS, like other watershed models, has not been designed or calibrated to accommodate spatially and daily varying cloud cover and insolation within the basins. The current experiment indicates that, with the advent of RNNCCS radiation products, modifications of the model to accommodate such inputs are in

order. They likely will yield their most significant improvements in models reformulated to accommodate directly the significant spatiotemporal variability illustrated by the RNNCCS products.

6. Additional opportunities: Areal extent of snow cover

Accumulation of snowpack in the Sierra Nevada during the winter provides the storage mechanism for water that later is released in the spring/early summer melt phase. At present, snow cover products provide a basis for recalibration and validation of models (e.g., Koczot and Dettinger 1999). Commonly used basin-scale streamflow models [e.g., the PRMS model for the Merced River basin (Fig. 11)], however, do not use the areal extent of snow cover as a direct input to the model. Rather, areal extent of snow cover is computed as an internal model variable based on a number of assumptions associated with accumulated model water and temperature balance over time. Snow water content is the primary snow characteristic simulated by models but is less amenable to high-frequency remote sensing at basin scales than is snow cover. Thus models that make more complete use of snow cover information will be a useful advance in the near future.

Hourly estimates of areal extent of snow cover, derived using the GOES-based retrieval method of Simpson and McIntire (2001), now make it possible to provide accurate estimates of areal extent of snow cover at 1-km spatial resolution and hourly temporal resolution on the same spatial grid as the GOES-based insolation estimates. This approach has several distinct advantages in comparison with current operational usage: 1) fixed relations among precipitation, air temperature, and areal extent of snow cover can be avoided; 2) the number of adjustable parameters/internal variables used in the models can be reduced; and 3) the tendency for operational models either to under- or overaccumulate water in model reservoirs can be reduced. In addition, the hourly resolution of GOES-based snow cover products allows for improvements in snow cover detection overall by making multiple classifications per day—each building from the one before—to be collated into daily consenses. Such consensus classifications provide new avenues for overcoming snow cover problems associated with the complex terrain and forest cover of the western United States.

In light of the improvements in snow cover classifications that have become possible, it is important to develop models that can employ such information to improve snowmelt simulations and streamflow forecasts. Such models are not yet available. In current watershed models, arbitrary adjustments of snow cover or snow water content to reflect remotely sensed snow patterns have long-term, far-reaching, and often unpredictable influences on the model performance and, unless done in ways that are very faithful to the real (but

unknown) distributions of water and snow in the basins, can greatly disrupt that performance. Indeed, the hardest part of incorporating such observations into ongoing simulations will be preservation of the constantly changing water balances in the basins while accommodating snow patterns from outside the models. When such balances are modified in even subtly incorrect ways, snow melts in the wrong places, at the wrong times, and in the wrong amounts, and the consequences for the modeler are both immediate and long lasting. However, when a model's snow cover is sufficiently far from the observed pattern, simple modifications to bring the model snowpack into agreement with the observations can help.

The dashed curves in Figs. 15b and 15d illustrate the results of simulations in which the initial snowpacks were modified to reflect RNNCCS-observed snow cover. In these examples, areas in the basins where snow cover was not observed but where it had existed in the unmodified initial conditions (which had previously been based on PRMS simulations leading up to the starting date of the RNNCCS observations) were simply stripped of all snow in the models. In the Merced River model, this revision of the initial snow cover resulted in a moderate decrease in streamflows throughout the simulation, because too much snow was removed by the simple process and thus was not available to contribute snowmelt and streamflow. The resulting simulation errors were quickly realized and persistent, yielding a slight increase in rms error as compared with the simulation with only basin-averaged RNNCCS insolation inputs (Table 3). In the Carson River, however, removing snow from areas that were not actually snow covered at the beginning of the simulation yielded a simulation that, although also tending to underestimate the flows, reproduced the tendency of the flows, from day 168 on, much more realistically than did the simulations with unmodified snow cover. The rms errors in the simulation with corrected initial snow cover are markedly improved in comparison with the other simulations (Table 3). These examples from 1998 only hint at the importance that snow cover may have in improving simulated flows, but they demonstrate the persistence and impact that such modifications will have on models that are better designed to accept such observations directly.

7. Advantages of new satellite products for hydrology

Robust retrievals of hydrologic basin model variables (e.g., insolation or areal extent of snow cover) provide several advantages over the current operational use of point measurements and model parameterizations. Insolation can be provided at hourly time scales (or better if needed—e.g., during rapid melt events associated with flooding) at 1-km spatial resolution. These satellite-based retrievals incorporate the effects of highly variable and unpredictable cloud cover on estimates of in-

solation. In situ measurements of insolation are very limited in extent and cannot capture the basinwide variability. The insolation estimates are further adjusted for the effects of basin topography using a high-resolution DEM prior to model input. Direct retrieval of areal extent of snow cover may mitigate the need to rely entirely on internal calculations of this variable, a reliance that can yield large errors that are difficult to correct until long after the season is complete and that often leads to underestimation or overestimation of the volume of the water in model reservoirs.

8. Conclusions

The streamflow simulations described here demonstrate that some streamflow fluctuations in these rivers reflect insolation variations that are not being captured in current operational parameterizations. These variations derive from the passage of clouds over the basins—clouds that are transitory and almost random in their effects and that can only be identified and quantified at basin scales by remote sensing approaches like the RNNCCS system used here. These clouds are of spatial scales that are comparable to the scales of the river basins, and, although generally smaller than those basins, the clouds interfere with insolation on areas that constitute significant fractions of the snowfields and drainages. The influences of these clouds are apparently separate from the large-scale fluctuations of temperature that are typically measured at weather stations used to force the models and commonly are not associated with precipitation. Therefore the influences of these clouds are not presently reaching current snowmelt models. Immediate gains in simulation skill were made when the effects of cloud variations were included in the models used here.

Further gains are to be expected if a new generation of models is designed to incorporate more such information, as well as more information about the evolution of snow cover in the basins. These new models should be more physically based than current operational models, which are highly parameterized. In addition to such new models, improvements in simulation skill by this approach will require establishment of an operational system to provide practitioners with access to real-time remotely sensed insolation and snow cover data, along the lines of the RNNCCS system described here, for input to river models. Beyond this, incorporation of such "new" information into river forecast models will require a ready stream of forecasts of insolation from existing weather-forecast sources. Insolation forecasts, added to the currently available temperature and precipitation forecasts, will make for better streamflow forecasts while also finding uses in many emerging technical areas such as ecosystem and cryospheric forecasting.

REFERENCES

Adams, J. B., M. O. Smith, and P. E. Johnson, 1986: Spectral mixing models: A new analysis of rock and soil types at the *Viking Lander 1* site. *J. Geophys. Res.,* **91,** 8098–8112.

Aguado, E., 1985: Radiation balances of melting snow covers at an open site in the central Sierra Nevada, California. *Water Resour. Res.,* **21,** 1649–1654.

Alpert, P., 1986: Mesoscale indexing of the distribution of the orographic precipitation over high mountains. *J. Climate Appl. Meteor.,* **25,** 532–545.

Armstrong, J. K., 1988: Topographic position effects on growth depression on California Sierra Nevada pines during the 1982–83 El Niño. *Arct. Alpine Res.,* **20,** 352–357.

Bales, R. C., and R. F. Harrington, 1995: Recent progress in snow hydrology. *Rev. Geophys.,* **33,** 1011–1020.

Betterton, M. D., 2001: Theory of structure formation in snowfields motivated by penitents, suncups, and dirt cones. *Phys. Rev.,* **E63,** 056129, doi:10.1103/PhysRevE.63.056192.

Beven, K., A. Calver, and E. N. Morris, 1987: Institute of Hydrology distributed model. Institute of Hydrology Internal Rep., Vol. 98, Wallingford, United Kingdom, 33 pp.

Blöschl, G., 1999: Scaling issues in snow hydrology. *Hydrol. Processes,* **13,** 2149–2175.

Cayan, D. R., and R. H. Webb, 1992: El Niño/Southern Oscillation and streamflow in the western United States. *El Niño: Historical and Paleoclimatic Aspects of the Southern Oscillation,* H. F. Diaz and V. Markgraf, Eds., Cambridge University Press, 26–68.

Colle, B. A., and C. F. Mass, 1996: An observational modeling study of the interaction of low-level southwesterly flow with the Olympic Mountains during COASTOP4. *Mon. Wea. Rev.,* **124,** 2152–2175.

Daly, C., R. P. Neilson, and D. L. Phillips, 1994: A statistical–topographic model for mapping climatological precipitation over mountainous terrain. *J. Appl. Meteor.,* **33,** 140–158.

Dettinger, M. D., K. Mo, D. R. Cayan, and D. H. Peterson, 1998: Hindcasts and forecasts of streamflow in the Merced and American Rivers, Sierra Nevada, during recent El Niños. *Eos, Trans. Amer. Geophys. Union,* **79** (Suppl.), F326.

——, D. R. Cayan, M. K. Meyer, and A. E. Jeton, 2004: Simulated hydrologic responses to climate variations and change in the Merced, Carson, and American River basins, Sierra Nevada, California, 1900–2099. *Climatic Change,* **62**.

Elder, K., W. Rosenthal, and R. E. Davis, 1998: Estimating the spatial distribution of snow water equivalence in a montane watershed. *Hydrol. Processes,* **12,** 1793–1808.

Greenland, D., and M. Losleben, 2001: Climate. *Structure and Function of an Alpine Ecosystem—Niwot Ridge, Colorado,* W. D. Bowman and T. R. Seastedt, Eds., Oxford University Press, 15–31.

Hardy, J. P., R. E. Davis, T. Pangburn, K. Elder, W. Rosenthal, and P. Pugner, 1998: Snow fraction mapping—Potential improvements to operational hydrologic forecasts. *Eos, Trans. Amer. Geophys. Union,* **79,** F271.

Harrington, R. F., and R. C. Bales, 1998: Interannual, seasonal, and

spatial patterns of meltwater and solute fluxes in a seasonal snowpack. *Water Resour. Res.,* **34,** 823–831.

Hay, L. E., and G. J. McCabe, 1998: Verification of the Rhea-orographic precipitation model. *J. Amer. Water Resour. Assoc.,* **34,** 103–112.

Hughes, N. A., and A. Henderson-Sellers, 1983: The effects of spatial and temporal averaging on sampling strategies for cloud amount data. *Bull. Amer. Meteor. Soc.,* **64,** 250–257.

Jeton, A. E., and J. L. Smith, 1993: The development of watershed models for two Sierra Nevada basins using a geographic information system. *Water Resour. Bull.,* **29,** 923–932.

——, M. D. Dettinger, and J. L. Smith, 1996: Potential effects of climate change on streamflow, eastern and western slopes of the Sierra Nevada, California and Nevada. U.S. Geological Survey Water Resources Investigations Rep. 95-4260, 44 pp.

Juang, H.-M. H., S.-Y. Hong, and M. Kanamitsu, 1997: The NCEP regional spectral model: An update. *Bull. Amer. Meteor. Soc.,* **78,** 2125–2143.

Kalnay, E., and Coauthors, 1996: The NCEP/NCAR 40-Year Reanalysis Project. *Bull. Amer. Meteor. Soc.,* **77,** 437–471.

Kattelman, R., and K. Elder, 1993: Accumulation and ablation of snow cover in an alpine basin in the Sierra Nevada, USA. *Snow and Glacier Hydrology,* G. J. Young, Ed., IAHS Press, 297–307.

Kimball, H. H., 1928: Amount of solar radiation that reaches the surface of the earth on the land and on the sea and methods by which it is measured. *Mon. Wea. Rev.,* **56,** 393–399.

Kirnbauer, R., G. Blöschl, and D. Gutknecht, 1994: Entering the era of distributed snow models. *Nord. Hydrol.,* **25,** 1–24.

Koczot, K. M., and M. D. Dettinger, 1999: Comparisons of simulated and remotely sensed snow-cover observations, Sierra Nevada. *Proc. 1999 Western Snow Conf.,* South Lake Tahoe, CA.

Komajda, R. J., and K. McKenzie, 1994: An introduction to the GOES I-M imager and sounder instruments and the GVAR retransmission format. NOAA Tech. Rep. NESDIS 82, Washington, DC, 56 pp.

Leavesley, G. H., R. W. Lichty, B. M. Troutman, and L. G. Saindon, 1983: Precipitation-runoff modeling system: User's manual. USGS Water Resources Investigations Rep. 83-4238, 207 pp.

Liniger, H., R. Weingartner, and M. Grosjean, 1998: *Mountains of the World—Water Towers for the 21st Century.* Paul Haupt AG, 32 pp.

Lohmann, D., E. Raschke, B. Nijssen, and D. P. Lettenmaier, 1998: Regional scale hydrology. I: Formulation of the VIC-2L model coupled to a routing model. *Hydrol. Sci. J.,* **43,** 131–142.

Lumb, F. E., 1964: The influence of cloud on hourly amount of total solar radiation at the sea surface. *Quart. J. Roy. Meteor. Soc.,* **90,** 43–56.

Lundquist, J. D., and D. R. Cayan, 2002: Seasonal and spatial patterns in diurnal cycles in streamflow in the western United States. *J. Hydrometeor.,* **3,** 591–603.

Mantua, N. J., S. R. Hare, Y. Zhang, J. M. Wallace, and R. C. Francis, 1997: A Pacific interdecadal climate oscillation with impacts on salmon production. *Bull., Amer. Meteor. Soc.,* **78,** 1069–1079.

Marks, D., J. Domingo, D. Susong, T. Link, and D. Garen, 1999: A spatially distributed energy balance snowmelt model for application in mountain basins. *Hydrol. Processes,* **13,** 1935–1959.

Mock, C. J., and K. W. Birkeland, 2000: Snow avalanche climatology of the western United States mountain ranges. *Bull. Amer. Meteor. Soc.,* **81,** 2367–2391.

Nakai, Y., T. Sakamoto, T. Terajima, K. Kitamura, and T. Shirai, 1999: The effect of canopy-snow on the energy balance above a coniferous forest. *Hydrol. Processes,* **13,** 2371–2383.

Obled, C., and B. B. Rosse, 1977: Mathematical models of a melting snowpack at an index plot. *J. Hydrol.,* **32,** 139–163.

Pandey, G. R., D. R. Cayan, and K. P. Georgakakos, 1999: Precipi-

tation structure in the Sierra Nevada of California during winter. *J. Geophys. Res.,* **104** (D10), 12 019–12 030.

——, ——, M. D. Dettinger, and K. P. Georgakakos, 2000: A hybrid orographic plus statistical model for downscaling daily precipitation in northern California. *J. Hydrometeor.,* **1,** 491–50.

Peterson, D. H., R. E. Smith, M. D. Dettinger, D. R. Cayan, and L. Riddle, 2000: An organized signal in snowmelt runoff over the western United States. *J. Amer. Water Resour. Assoc.,* **36,** 421–432.

Planet, W. G., 1988: Data extraction and calibration of TIROS-N/NOAA radiometers. NOAA Tech. Memo NESS 107 (Rev. 1), Washington, DC, 119 pp.

Robinson, D. E., and K. F. Dewey, 1990: Recent secular variations in the extent of Northern Hemisphere snow cover. *Geophys. Res. Lett.,* **17,** 1557–1560.

Rossow, W. B., 1993: Clouds. *Atlas of Satellite Observations Related to Global Change,* R. J. Gurney, J. L. Foster, and C. L. Parkinson, Eds., Cambridge University Press, 141–163.

Sayliegh, A. A. M., 1977: *Solar Energy Engineering.* Academic Press, 506 pp.

Sellers, W. D., 1965: *Physical Climatology.* The University of Chicago Press, 272 pp.

Sèze, G., and W. B. Rossow, 1991: Time-cumulated visible and infrared radiance histograms used as descriptors of surface and cloud variations. *Int. J. Remote Sens.,* **12,** 921–952.

Simpson, J. J., 1992: Image masking using polygon fill and morphological operations. *Remote Sens. Environ.,* **40,** 161–183.

——, and C. A. Paulson, 1979: Mid-ocean observations of atmospheric radiation. *Quart. J. Roy. Meteor. Soc.,* **105,** 487–502.

——, and J. R. Stitt, 1998: A procedure for the detection and removal of cloud shadow from AVHRR data over land. *IEEE Trans. Geosci. Remote Sens.,* **36,** 880–897.

——, and T. J. McIntire, 2001: Accurate detection of areal extent of snow cover in satellite data using neural networks. *IEEE Trans. Geosci. Remote Sens.,* **39,** 2135–2147.

——, Z. Jin, and J. R. Stitt, 2000: Cloud shadow detection under arbitrary viewing and illumination conditions. *IEEE Trans. Geosci. Remote Sens.,* **38,** 972–976.

Tarboton, D. G., T. G. Chowdhury, and T. H. Jackson, 1995: A spatially distributed energy balance snowmelt model. *Biogeochemistry of Seasonally Snow-Covered Catchments,* K. A. Tonnessen, Ed., IAHS Publ. 228, 141–155.

Walker, M. D., D. A. Walker, T. A. Theodose, and P. J. Webber, 2001: The vegetation–hierarchical species–environment relationships. *Structure and function of an Alpine Ecosystem—Niwot Ridge, Colorado,* W. D. Bowman and T. R. Seastodt, Oxford University Press, 99–127.

Welch, R. M., K. S. Kuo, B. A. Wielicki, S. K. Sengupta, and L. Parker, 1988: Marine stratocumulus cloud fields off the coast of southern California observed using LANDSAT imagery. Part I: Structural characteristics. *J. Appl. Meteor.,* **27,** 363–378.

Wilby, R. L., and M. D. Dettinger, 2000: Streamflow changes in the Sierra Nevada, California, simulated using statistically downscaled general circulation model output. *Linking Climate Change to Land Surface Change,* S. McLaren and D. Kniveton, Eds., Kluwer Academic, 99–121.

Willen, D. W., C. A. Shumway, and J. E. Reid, 1971: Simulation of daily snow water equivalent and melt. *Proc. 1971 Western Snow Conf.,* Billings, MT, Vol. 39, 1–8.

Winther, J. G., and D. K. Hall, 1999: Satellite-derived snow coverage related to hydropower production in Norway—Present and future. *Int. J. Remote Sens.,* **20,** 2991–3008.

World Meteorological Organization, 1956: *International Cloud Atlas.* Vol. 1. WMO, 155 pp.

——, 1986: Intercomparison of models of snowmelt runoff. World Meteorological Organization Operational Hydrology Rep. 23, WMO Publ. 646, 430 pp.